

# A fully conservative and shift-invariant formulation for Galerkin discretizations of incompressible variable density flow

Lukas Lundgren<sup>a,\*</sup>, Murtazo Nazarov<sup>a</sup>

<sup>a</sup>*Department of Information Technology, Division of Scientific Computing, Uppsala University, Sweden*

---

## Abstract

This paper introduces a formulation of the variable density incompressible Navier-Stokes equations by modifying the nonlinear terms in a consistent way. For Galerkin discretizations, the formulation leads to full discrete conservation of mass, squared density, momentum, angular momentum and kinetic energy without the divergence-free constraint being strongly enforced. In addition to favorable conservation properties, the formulation is shown to make the density field invariant to global shifts. The effect of viscous regularizations on conservation properties is also investigated. Numerical tests validate the theory developed in this work. The new formulation shows superior performance compared to other formulations from the literature, both in terms of accuracy for smooth problems and in terms of robustness.

*Keywords:* incompressible variable density flow, Navier-Stokes equations, conservation, EMAC formulation, viscous regularization, angular momentum

---

## 1. Introduction.

The simulation of incompressible flow is important for industrial and scientific applications when modeling subsonic flow. In this work, we consider incompressible flow when the density field is variable, which is the case for fluids with distinct phases, i.e., air and carbon dioxide, oil and water and so on. The governing equations we consider are the incompressible Navier-Stokes equations with variable density augmented with an advection equation for the density field. At the continuous level, the equations can be shown to conserve mass, squared density, momentum, angular momentum and kinetic energy. The density field can also be shown to be shift-invariant which means that density remains invariant if it is shifted by a constant. These properties are fundamental to the flow model and are closely linked to the so-called divergence-free constraint which is pointwise satisfied. It is favorable for numerical approximations of variable density flow to fulfill as many of these physical properties as possible.

Unfortunately, numerical approximations of the incompressible Navier-Stokes equations are rarely pointwise divergence-free [19] which leads to issues with conservation. In particular, most Galerkin methods are known to satisfy the divergence-free condition only weakly and much work has been performed to improve the conservation properties of these methods. Recently, Charnyi et al. [5] showed that, by consistently modifying the nonlinear term in the constant density Navier-Stokes equations, a fully conservative Galerkin method could be derived. The novelty of the formulation is that a modified pressure is solved for and the formulation has been named the energy, momentum and angular momentum conserving (EMAC) formulation. The EMAC formulation has later been extended to be more efficient by Charnyi et al. [6], further analyzed by Olshanskii and Rebholz [24] and extended to projection methods by Ingimarson et al. [16].

Unlike constant density flow, variable density flow has additional conserved properties and no fully conservative formulation is currently known in the literature. The current state-of-the-art formulations for

---

\*Corresponding author

*Email addresses:* lukas.lundgren@it.uu.se (Lukas Lundgren), murtazo.nazarov@it.uu.se (Murtazo Nazarov)

variable density flow are based on skew-symmetric formulations that can be shown to conserve squared density and kinetic energy [13] or a formulation that can be shown to conserve mass, kinetic energy, momentum and angular momentum [29, 21]. In this work, we extend the modified pressure technique [5] to variable density flow which leads to a new formulation that, when discretized by a Galerkin method, is shift-invariant and also conserves mass, squared density, kinetic energy, momentum and angular momentum. The analysis is first performed on the inviscid problem, i.e., the incompressible Euler equations with variable density. Later, since viscous regularizations affect the conservation properties of the model, we also investigate this.

The theoretical findings are summarized in Theorems 3.1 and 4.1, and these are verified using numerical experiments. The results show that the new formulation leads to improved accuracy and robustness compared to existing formulations in the variable density literature. Furthermore, the new formulation can easily be implemented into existing Galerkin-based variable density Navier-Stokes solvers.

The paper is organized the following way: In Section 2 we give the governing equations, present our notation and explain the properties of the governing equations that we later want our proposed numerical method to mimic. Then, in Section 3 we introduce an alternative formulation of the governing equations which, when discretized using a Galerkin method, leads to improved conservation properties in the semi-discrete form. In Section 4 we present a family of viscous regularizations that lead to various conserved properties of the model. In Section 5 a conservative second-order accurate time discretization is presented which leads to a fully discrete method. In Section 6 we perform numerical validations. In Section 7 we give concluding remarks.

## 2. Preliminaries.

In this section, we introduce the governing equations that model variable density flow. We start with the inviscid case, i.e., we only consider the incompressible Euler equations with variable density. We also discuss the properties of the governing equations and present our notation.

### 2.1. The inviscid model problem.

We first consider the incompressible Euler equations with variable density in a domain  $\Omega \subset \mathbb{R}^d$  where  $d$  is the dimension and with finite time interval  $[0, T]$

$$\begin{aligned} \partial_t \rho + \mathbf{u} \cdot \nabla \rho &= 0, \\ \partial_t \mathbf{m} + \mathbf{u} \cdot \nabla \mathbf{m} + \nabla p &= \mathbf{f}, & (\mathbf{x}, t) \in \Omega \times (0, T], \\ \nabla \cdot \mathbf{u} &= 0, & \mathbf{x} \in \Omega, \\ \mathbf{u}(\mathbf{x}, 0) &= \mathbf{u}_0(\mathbf{x}), & \mathbf{x} \in \Omega, \\ \rho(\mathbf{x}, 0) &= \rho_0(\mathbf{x}), \end{aligned} \tag{2.1}$$

where the density  $\rho > 0$ , the velocity field  $\mathbf{u}$  and the pressure  $p$  are the unknowns. We define  $\mathbf{m} := \rho \mathbf{u}$  as the momentum vector,  $\mathbf{f}(\mathbf{x}, t)$  represents an external force,  $\rho_0(\mathbf{x})$ ,  $\mathbf{u}_0(\mathbf{x})$  are initial conditions for density and velocity. We assume that the governing equations are supplied with well-posed boundary conditions. To simplify the analysis we set  $\mathbf{f} = 0$  and consider periodic boundary conditions.

**Remark 2.1.** It is possible to write the governing equations in primitive form, i.e.,  $\rho \mathbf{u}_t + \mathbf{m} \cdot \nabla \mathbf{u}$  instead of  $\mathbf{m}_t + \mathbf{u} \cdot \nabla \mathbf{m}$ . All of the results presented in this manuscript can straightforwardly be extended to this form. See [Appendix A](#) for more details.

### 2.2. Notation and useful identities.

Let  $\rho, w \in H^1(\Omega)$  and  $\mathbf{u}, \mathbf{w}, \mathbf{v}, \mathbf{m} \in \mathbf{H}^1(\Omega) := [H^1(\Omega)]^d$ . In this work the  $L^2$  inner product is written as  $(\cdot, \cdot)$  with associated  $L^2$  norms  $\|\cdot\|$  and we define  $(\nabla \mathbf{u}) := \partial_{x_i} u_j$ . We also define a trilinear form

$$b(\mathbf{u}, \mathbf{v}, \mathbf{w}) := (\mathbf{u} \cdot \nabla \mathbf{v}, \mathbf{w}) = ((\nabla \mathbf{v})^\top \mathbf{u}, \mathbf{w}) = ((\nabla \mathbf{v}) \mathbf{w}, \mathbf{u}). \tag{2.2}$$

The following identities hold:

$$b(\mathbf{u}, \mathbf{m}, \mathbf{v}) = b(\mathbf{m}, \mathbf{u}, \mathbf{v}) + (\mathbf{u} \cdot \nabla \rho, \mathbf{u} \cdot \mathbf{v}), \quad (2.3)$$

$$b(\mathbf{u}, \mathbf{u}, \mathbf{m}) = b(\mathbf{m}, \mathbf{u}, \mathbf{u}), \quad (2.4)$$

where (2.3) follows from  $\mathbf{u} \cdot \nabla(\rho \mathbf{u}) = \rho \mathbf{u} \cdot \nabla \mathbf{u} + (\mathbf{u} \cdot \nabla \rho) \mathbf{u}$  and (2.4) follows from the definition of the trilinear form (2.2).

Since the domain is periodic the following relations hold due to integration by parts

$$b(\mathbf{u}, \mathbf{v}, \mathbf{w}) = -b(\mathbf{u}, \mathbf{w}, \mathbf{v}) - ((\nabla \cdot \mathbf{u}) \mathbf{v}, \mathbf{w}), \quad (2.5)$$

$$b(\mathbf{u}, \mathbf{w}, \mathbf{w}) = -\frac{1}{2}((\nabla \cdot \mathbf{u}) \mathbf{w}, \mathbf{w}), \quad (2.6)$$

$$(\mathbf{u} \cdot \nabla \rho, \mathbf{w}) = -(\mathbf{u} \cdot \nabla \mathbf{w}, \rho) - ((\nabla \cdot \mathbf{u}) \rho, \mathbf{w}), \quad (2.7)$$

$$(\mathbf{u} \cdot \nabla \rho, \rho) = -\frac{1}{2}((\nabla \cdot \mathbf{u}) \rho, \rho). \quad (2.8)$$

We also define  $\mathbf{e}_i$  as a unit vector, i.e., in 3D  $\mathbf{e}_1 = (1, 0, 0)^\top$ ,  $\mathbf{e}_2 = (0, 1, 0)^\top$  and  $\mathbf{e}_3 = (0, 0, 1)^\top$ . We define  $\boldsymbol{\phi}_i := \mathbf{x} \times \mathbf{e}_i$  and note that  $\boldsymbol{\phi}_i$  has the property that  $\nabla \cdot \boldsymbol{\phi} = 0$  and  $\nabla \boldsymbol{\phi}_i + (\nabla \boldsymbol{\phi}_i)^\top = 0$ . To get a correct definition of the cross product in 2D, the last component of all the vectors is extended by 0.

### 2.2.1. Finite element preliminaries.

We denote a shape regular computational mesh by  $\mathcal{T}_h$  which is a triangulation of  $\Omega$  into a finite number of disjoint elements  $K$ . We define the following finite element spaces

$$\mathcal{M} := \{w(\mathbf{x}) : w \in \mathcal{C}^0(\Omega), w|_K \in \mathbb{P}_{k_\rho}, \forall K \in \mathcal{T}_h\},$$

$$\mathcal{V} := \left[ \{v(\mathbf{x}) : v \in \mathcal{C}^0(\Omega), v|_K \in \mathbb{P}_{k_u}, \forall K \in \mathcal{T}_h\} \right]^d,$$

$$\mathcal{Q} := \left\{ q(\mathbf{x}) : q \in \mathcal{C}^0(\Omega), q|_K \in \mathbb{P}_{k_P}, \forall K \in \mathcal{T}_h, \int_\Omega q \, d\mathbf{x} = 0 \right\},$$

where  $\mathbb{P}_{k_\rho}, \mathbb{P}_{k_u}, \mathbb{P}_{k_P}$  are the set of multivariate polynomials of total degree at most  $k_\rho, k_u, k_P \geq 1$  defined over  $K$ . It is well-known that to satisfy the so-called inf-sup condition [9] we require  $k_P < k_u$ . The corresponding discrete inner products are defined as

$$(v, w) := \sum_{K \in \mathcal{T}_h} \int_K v w \, d\mathbf{x}, \quad (\mathbf{v}, \mathbf{w}) := \sum_{K \in \mathcal{T}_h} \int_K \mathbf{v} \cdot \mathbf{w} \, d\mathbf{x}, \quad (\nabla \mathbf{v}, \nabla \mathbf{w}) := \sum_{K \in \mathcal{T}_h} \int_K \nabla \mathbf{v} : \nabla \mathbf{w} \, d\mathbf{x},$$

with associated  $L^2$  norms  $\|\cdot\|$ . Discrete and continuous inner products are used interchangeably for brevity. The discrete mesh size function  $h(\mathbf{x})$  is constructed as the following continuous piece-wise linear function: for every nodal point  $N_i$

$$h(N_i) := \min(h_K / \max(k_u, k_\rho), \quad \forall K \in \mathcal{T}_h \text{ such that } N_i \in K)$$

where  $h_K$  is the smallest edge of  $K$ .

### 2.3. Properties of the governing equations.

The governing equations can be shown to conserve mass, squared density, kinetic energy, momentum and angular momentum. These are defined as

$$\begin{aligned} \text{Mass} & \int_\Omega \rho \, d\mathbf{x}; & \text{Kinetic energy} & \frac{1}{2} \int_\Omega \rho \mathbf{u} \cdot \mathbf{u} \, d\mathbf{x}; & \text{Angular momentum} & \int_\Omega \mathbf{m} \times \mathbf{x} \, d\mathbf{x}; \\ \text{Momentum} & \int_\Omega \mathbf{m} \, d\mathbf{x}; & \text{Squared density} & \frac{1}{2} \int_\Omega \rho^2 \, d\mathbf{x}. \end{aligned}$$

Another property that is rarely (if at all) mentioned in the variable density flow literature is that the mass equation is invariant to shifts in the density field. A more precise definition is given below:

**Definition 2.1.** If  $\rho$  is shifted by a constant  $c$ , then the mass equation remains invariant to this change, i.e., it holds that

$$\partial_t \rho + \mathbf{u} \cdot \nabla \rho = 0 \quad \Leftrightarrow \quad \partial_t(\rho + c) + \mathbf{u} \cdot \nabla(\rho + c) = 0.$$

### 3. Properties when $\nabla \cdot \mathbf{u} \neq 0$ .

For most numerical methods,  $\nabla \cdot \mathbf{u} = 0$  does not hold pointwise at the discrete level. This is also true for most Galerkin methods where the numerical solution usually satisfies

$$(\nabla \cdot \mathbf{u}, q) = 0, \quad \forall q \in Q.$$

We note that there are some exceptions to this. In particular, some exotic elements are pointwise divergence-free such as iso-geometric B-splines [7], Raviart-Thomas elements [26, 8], Scott-Vogelius elements [27] and so on, but some of these are not included in all FEM software libraries and some introduce constraints on the computational mesh and polynomial degree. Additionally, not all divergence-free elements, such as [26, 8], are  $H^1$ -conforming which is a favorable property to have.

In this work, we analyze many variations of the nonlinear terms. Depending on how these are chosen, favorable conservation properties can be obtained which we investigate thoroughly in this work. To this end, we write the governing equations (2.1) in a more general form

$$\begin{aligned} \partial_t \rho + \mathbf{u} \cdot \nabla \rho + \alpha_\rho (\nabla \cdot \mathbf{u}) \rho &= 0, \\ \partial_t \mathbf{m} + \mathbf{u} \cdot \nabla \mathbf{m} + \alpha_m (\nabla \cdot \mathbf{u}) \mathbf{m} + \nabla P + \alpha_P (\nabla \mathbf{u}) \mathbf{m} + \alpha_P (\nabla \mathbf{m}) \mathbf{u} &= 0, \end{aligned} \quad (3.1)$$

where  $P = p - \alpha_P \mathbf{u} \cdot \mathbf{m}$  is a modified pressure and  $\alpha_\rho, \alpha_m, \alpha_P \in \mathbb{R}$ . The terms involving  $\nabla \cdot \mathbf{u}$  are consistent with the governing equations and have previously been used for variable density flow in different variations to derive numerical methods, see e.g., [13, 25, 3, 1, 29]. The modified pressure technique ( $\alpha_P \neq 0$ ) has been successfully applied for constant density flow [5] but has currently not been applied in the variable density context. Depending on how  $\alpha_\rho, \alpha_m, \alpha_P$  are chosen different conservation properties are obtained. By using that  $(\nabla \mathbf{m}) \mathbf{u} = (\nabla(\rho \mathbf{u})) \mathbf{u} = (\nabla \rho \otimes \mathbf{u}) \mathbf{u} + (\nabla \mathbf{u}) \rho \mathbf{u} = \nabla \rho (\mathbf{u} \cdot \mathbf{u}) + (\nabla \mathbf{u}) \mathbf{m}$ , the system (3.1) can equivalently be expressed as

$$\begin{aligned} \partial_t \rho + \mathbf{u} \cdot \nabla \rho + \alpha_\rho (\nabla \cdot \mathbf{u}) \rho &= 0, \\ \partial_t \mathbf{m} + \mathbf{u} \cdot \nabla \mathbf{m} + \alpha_m (\nabla \cdot \mathbf{u}) \mathbf{m} + \nabla P + \left( \alpha_P + \frac{1}{2} \right) (\nabla \mathbf{u}) \mathbf{m} \\ + \left( \alpha_P - \frac{1}{2} \right) (\nabla \mathbf{m}) \mathbf{u} + \frac{1}{2} ((\mathbf{u} \cdot \mathbf{u}) \nabla \rho - \alpha_\rho \nabla(\rho \mathbf{u} \cdot \mathbf{u})) + \frac{1}{2} \alpha_\rho \nabla(\rho \mathbf{u} \cdot \mathbf{u}) &= 0, \end{aligned}$$

Lastly, we introduce  $\bar{\rho} \in \mathbb{R}$  which, if properly chosen, will make the system below shift-invariant

$$\begin{aligned} \partial_t \rho + \mathbf{u} \cdot \nabla \rho + \alpha_\rho (\nabla \cdot \mathbf{u}) (\rho - \bar{\rho}) &= 0, \\ \partial_t \mathbf{m} + \mathbf{u} \cdot \nabla \mathbf{m} + \alpha_m (\nabla \cdot \mathbf{u}) \mathbf{m} + \nabla P + \left( \alpha_P + \frac{1}{2} \right) (\nabla \mathbf{u}) \mathbf{m} \\ + \left( \alpha_P - \frac{1}{2} \right) (\nabla \mathbf{m}) \mathbf{u} + \frac{1}{2} (\nabla \rho (\mathbf{u} \cdot \mathbf{u}) - \alpha_\rho \nabla((\rho - \bar{\rho}) \mathbf{u} \cdot \mathbf{u})) + \frac{1}{2} \alpha_\rho \nabla(\rho \mathbf{u} \cdot \mathbf{u}) &= 0, \end{aligned} \quad (3.2)$$

where  $P = p - \alpha_P \rho \mathbf{u} \cdot \mathbf{u} - \frac{1}{2} \alpha_\rho \bar{\rho} \mathbf{u} \cdot \mathbf{u}$  is a modified pressure which now includes  $\bar{\rho}$ . To the best of the authors' knowledge, using  $\bar{\rho}$  to achieve shift-invariant formulations is new to the literature for both variable density flow and scalar transport problems in general.

### 3.1. Galerkin finite element approximation.

The finite element approximation of (3.2) is derived by testing the mass equation with  $w$ , the momentum equations with  $\mathbf{v}$  and the divergence-free constraint with  $q$ . The finite element method reads: Find  $(\rho, \mathbf{u}, P) \in (\mathcal{M}, \mathcal{V}, \mathcal{Q})$  such that

$$\begin{aligned}
& (\rho_t, w) + (\mathbf{u} \cdot \nabla \rho, w) + \alpha_\rho ((\nabla \cdot \mathbf{u})(\rho - \bar{\rho}), w) = 0, \quad \forall w \in \mathcal{M}, \\
& (\mathbf{m}_t, \mathbf{v}) + b(\mathbf{u}, \mathbf{m}, \mathbf{v}) + \alpha_m ((\nabla \cdot \mathbf{u})\mathbf{m}, \mathbf{v}) + (\nabla P, \mathbf{v}) \\
& + \left( \alpha_P - \frac{1}{2} \right) b(\mathbf{v}, \mathbf{m}, \mathbf{u}) + \left( \alpha_P + \frac{1}{2} \right) b(\mathbf{v}, \mathbf{u}, \mathbf{m}) + \frac{1}{2} \alpha_\rho (\nabla(\mathbf{m} \cdot \mathbf{u}), \mathbf{v}) \\
& + \frac{1}{2} ((\mathbf{v} \cdot \nabla \rho, \overline{\mathbf{u} \cdot \mathbf{u}}) - \alpha_\rho (\nabla((\rho - \bar{\rho})\overline{\mathbf{u} \cdot \mathbf{u}}), \mathbf{v})) = 0, \quad \forall \mathbf{v} \text{ in } \mathcal{V}, \\
& (\nabla \cdot \mathbf{u}, q) = 0, \quad \forall q \in \mathcal{Q},
\end{aligned} \tag{3.3}$$

where  $\overline{\mathbf{u} \cdot \mathbf{u}} \in \mathcal{M}$  is the projection of  $\mathbf{u} \cdot \mathbf{u}$  onto  $\mathcal{M}$ , see e.g., Gawlik and Gay-Balmaz [8, Remark 3.1]: Find  $\overline{\mathbf{u} \cdot \mathbf{u}} \in \mathcal{M}$  such that

$$(\overline{\mathbf{u} \cdot \mathbf{u}}, w) = (\mathbf{u} \cdot \mathbf{u}, w), \quad \forall w \in \mathcal{M}. \tag{3.4}$$

The reason why  $\overline{\mathbf{u} \cdot \mathbf{u}}$  is used is that we later need to set  $w = \mathbf{u} \cdot \mathbf{u}$  to obtain a kinetic energy estimate. This means that we either need to project  $\mathbf{u} \cdot \mathbf{u}$  to  $\mathcal{M}$  (3.4) or we require  $k_\rho \geq 2k_u$ .

### 3.2. Semi-discrete properties of the Galerkin method.

We summarize the properties of the semi-discrete method (3.3) in Table 1 and Theorem 3.1 which is the main result of this work. In the constant density case, there exists a unique parameter choice such that kinetic energy, momentum and angular momentum are all conserved which has been named the EMAC formulation [5]. In the variable density context, we require additional constraints to achieve all properties in Table 1. All properties are achieved by setting  $\alpha_\rho = \frac{1}{2}, \alpha_m = 1, \alpha_P = 0.25, \bar{\rho} = \frac{1}{|\Omega|} \int_\Omega \rho \, d\mathbf{x}$  and by choosing the polynomial degree of density to be less than or equal to that of pressure ( $k_\rho \leq k_P$ ). This leads to a formulation that is shift-invariant and mass, kinetic energy, squared density, momentum and angular momentum conserving (SI-MEDMAC). If other parameter choices  $\alpha_\rho, \alpha_m, \alpha_P, \bar{\rho}, k_\rho$  are considered, we end up with common formulations from the variable density flow literature and several new ones, see Table 2. We follow a similar naming convention for the other formulations in Table 2, i.e., MEMAC is mass, kinetic energy, momentum, angular momentum conserving, EDMAC is kinetic energy, squared density, momentum, angular momentum conserving and so on. All formulations with  $\alpha_\rho = 0$  are, for a lack of a better term, named *locally* shift-invariant. If the domain is stretched, these formulations are invariant to this change but the other formulations are not. The convective form is the form that is obtained when (2.1) is discretized directly without any modifications.

Table 1: Semi-discrete properties of the method (3.3) when  $\mathbf{f} = 0$  for the inviscid case when  $\nabla \cdot \mathbf{u} \neq 0$ .

| Property  | Condition   |
|---|---|
| $\partial_t \int_\Omega \rho \mathbf{u} \cdot \mathbf{u} \, d\mathbf{x} = 0$  | $\alpha_m - \alpha_P - \alpha_\rho/2 = 1/2$   |
| $\partial_t \int_\Omega \mathbf{m} \, d\mathbf{x} = 0$  | $\alpha_m = 1$  |
| $\partial_t \int_\Omega \mathbf{m} \times \mathbf{x} \, d\mathbf{x} = 0$  | $\alpha_m = 1$  |
| $\partial_t \frac{1}{2} \int_\Omega \rho^2 \, d\mathbf{x} - \int_\Omega \bar{\rho} \partial_t \rho \, d\mathbf{x} = 0$                  | $\alpha_\rho = 1/2$   |
| $\partial_t \left( \int_\Omega \rho^2 \, d\mathbf{x} - \frac{1}{ \Omega } \left( \int_\Omega \rho \, d\mathbf{x} \right)^2 \right) = 0$ | $\alpha_\rho = 1/2$ and $\bar{\rho} = \frac{1}{ \Omega } \int_\Omega \rho \, d\mathbf{x}$     |
| $\partial_t \int_\Omega \rho^2 \, d\mathbf{x} = 0$  | $[\alpha_\rho = 1/2 \text{ and } k_\rho \leq k_P] \text{ or } 2k_\rho \leq k_P$               |
| $\partial_t \int_\Omega \rho \, d\mathbf{x} = 0$  | $k_\rho \leq k_P \text{ or } \alpha_\rho = 1$   |
| Shift invariance  | $\alpha_\rho = 0 \text{ or } \bar{\rho} = \frac{1}{ \Omega } \int_\Omega \rho \, d\mathbf{x}$ |

Table 2: Existing formulations in the literature and newly derived formulations for variable density flow. The formulations are later tested and compared in numerical experiments.

| Name                   | $\alpha_\rho$ | $\alpha_m$ | $\alpha_P$ | $\bar{\rho}$  | $k_\rho$          |
|------------------------|---------------|------------|------------|---|-------------------|
| LSI-EMAC               | 0             | 1          | 0.5        | N/A   | $\forall k_\rho$  |
| MEMAC [29, 21]         | 1             | 1          | 0          | 0   | $\forall k_\rho$  |
| EDMAC                  | 0.5           | 1          | 0.25       | 0   | $\forall k_\rho$  |
| SI-MEMAC               | 1             | 1          | 0          | $\bar{\rho} = \frac{1}{ \Omega } \int_\Omega \rho \, d\mathbf{x}$ | $\forall k_\rho$  |
| SI-EDMAC               | 0.5           | 1          | 0.25       | $\bar{\rho} = \frac{1}{ \Omega } \int_\Omega \rho \, d\mathbf{x}$ | $\forall k_\rho$  |
| SI-MEDMAC              | 0.5           | 1          | 0.25       | $\bar{\rho} = \frac{1}{ \Omega } \int_\Omega \rho \, d\mathbf{x}$ | $k_\rho \leq k_P$ |
| LSI-EC [20]            | 0             | 0.5        | 0          | N/A   | $\forall k_\rho$  |
| Convective [14, Sec 4] | 0             | 0          | 0          | N/A   | $\forall k_\rho$  |

**Theorem 3.1.** *The properties of Table 1 hold provided that the conditions inside it are met.*

*Proof.* We divide the proof into several parts. To simplify the proof we assume a periodic domain and set  $\mathbf{f} = 0$ . Extending the proofs to other boundary conditions such as no-slip ( $\mathbf{u} = 0|_{\partial\Omega}$ ) can be done by using the proof technique in [5, Sec 3.1.2] or [16, Sec 3.1.2].

**Mass:** By using the definition we have that (3.3) satisfies

$$\partial_t \int_\Omega \rho \, d\mathbf{x} = \int_\Omega \partial_t \rho \, d\mathbf{x} = -(\mathbf{u}, \nabla \rho) - \alpha_\rho (\nabla \cdot \mathbf{u}, \rho - \bar{\rho}). \quad (3.5)$$

Since  $\nabla \bar{\rho} = 0$ , (3.5) is equivalent to

$$\begin{aligned} \partial_t \int_\Omega \rho \, d\mathbf{x} &= -(\mathbf{u}, \nabla(\rho - \bar{\rho})) - \alpha_\rho (\nabla \cdot \mathbf{u}, \rho - \bar{\rho}) \\ &= (\nabla \cdot \mathbf{u}, \rho - \bar{\rho}) - \alpha_\rho (\nabla \cdot \mathbf{u}, \rho - \bar{\rho}) \\ &= (1 - \alpha_\rho) (\nabla \cdot \mathbf{u}, \rho - \bar{\rho}), \end{aligned}$$

where integration by parts was used on the first term. Therefore mass is conserved if  $\alpha_\rho = 1$ . If  $\bar{\rho} = \int_\Omega \rho \, d\mathbf{x}$  then

$$\int_\Omega \rho - \bar{\rho} \, d\mathbf{x} = 0,$$

which means that  $(\rho - \bar{\rho}) \in \mathcal{Q}$  provided that  $k_\rho \leq k_P$ . Invoking the weak divergence-free condition (3.3) shows that

$$(\nabla \cdot \mathbf{u}, \rho - \bar{\rho}) = 0,$$

which means that mass is conserved if  $k_\rho \leq k_P$ .

**Shift-invariance:** If  $\alpha_\rho = 0$  then the proof is evident from Definition 2.1. Otherwise, if  $\bar{\rho} = \frac{1}{|\Omega|} \int_\Omega \rho \, d\mathbf{x}$ , the following is obtained by shifting  $\rho$  by a constant  $c$  in (3.2)

$$\begin{aligned} \partial_t(\rho + c) + \mathbf{u} \cdot \nabla(\rho + c) + \alpha_\rho (\nabla \cdot \mathbf{u}) \left( \rho + c - \frac{1}{|\Omega|} \int_\Omega (\rho + c) \, d\mathbf{x} \right) &= 0, \\ \partial_t \rho + \mathbf{u} \cdot \nabla \rho + \alpha_\rho (\nabla \cdot \mathbf{u}) \left( \rho + c - \frac{1}{|\Omega|} \int_\Omega (\rho + c) \, d\mathbf{x} \right) &= 0, \\ \partial_t \rho + \mathbf{u} \cdot \nabla \rho + \alpha_\rho (\nabla \cdot \mathbf{u}) \left( \rho - \frac{1}{|\Omega|} \int_\Omega \rho \, d\mathbf{x} \right) &= 0, \\ \partial_t \rho + \mathbf{u} \cdot \nabla \rho + \alpha_\rho (\nabla \cdot \mathbf{u}) (\rho - \bar{\rho}) &= 0, \end{aligned}$$

which shows that the formulation is shift-invariant.

**Squared density:** By using that  $\nabla \bar{\rho} = 0$ , one can show that (3.3) satisfies

$$\partial_t \frac{1}{2} \int_{\Omega} \rho^2 \, d\mathbf{x} - \int_{\Omega} \bar{\rho} \partial_t \rho \, d\mathbf{x} = (\rho_t, \rho - \bar{\rho}) = -(\mathbf{u} \cdot \nabla (\rho - \bar{\rho}), \rho - \bar{\rho}) - \alpha_{\rho} ((\nabla \cdot \mathbf{u})(\rho - \bar{\rho}), \rho - \bar{\rho}). \quad (3.6)$$

Using (2.8) inside (3.6) yields

$$\partial_t \frac{1}{2} \int_{\Omega} \rho^2 \, d\mathbf{x} - \int_{\Omega} \bar{\rho} \partial_t \rho \, d\mathbf{x} = \left( \frac{1}{2} - \alpha_{\rho} \right) ((\nabla \cdot \mathbf{u})(\rho - \bar{\rho}), \rho - \bar{\rho}). \quad (3.7)$$

If  $\alpha_{\rho} = \frac{1}{2}$  then  $\partial_t \frac{1}{2} \int_{\Omega} \rho^2 \, d\mathbf{x} - \int_{\Omega} \bar{\rho} \partial_t \rho \, d\mathbf{x} = 0$ . This shows that line 4 in Table 1 is true.

If  $\bar{\rho} = \frac{1}{|\Omega|} \int_{\Omega} \rho \, d\mathbf{x}$ , then we can perform the following simplification

$$\begin{aligned} \partial_t \frac{1}{2} \int_{\Omega} \rho^2 \, d\mathbf{x} - \int_{\Omega} \bar{\rho} \partial_t \rho \, d\mathbf{x} &= \partial_t \frac{1}{2} \int_{\Omega} \rho^2 \, d\mathbf{x} - \bar{\rho} \int_{\Omega} \partial_t \rho \, d\mathbf{x} \\ &= \partial_t \frac{1}{2} \int_{\Omega} \rho^2 \, d\mathbf{x} - \frac{1}{|\Omega|} \left( \int_{\Omega} \rho \, d\mathbf{x} \right) \int_{\Omega} \partial_t \rho \, d\mathbf{x} \\ &= \partial_t \frac{1}{2} \int_{\Omega} \rho^2 \, d\mathbf{x} - \frac{1}{|\Omega|} \left( \int_{\Omega} \rho \, d\mathbf{x} \right) \partial_t \left( \int_{\Omega} \rho \, d\mathbf{x} \right) \\ &= \partial_t \frac{1}{2} \left( \int_{\Omega} \rho^2 \, d\mathbf{x} - \frac{1}{|\Omega|} \left( \int_{\Omega} \rho \, d\mathbf{x} \right)^2 \right), \end{aligned} \quad (3.8)$$

to show that line 5 in Table 1 is true.

Lastly, we consider line 6 in Table 1. By recalling that  $\partial_t \int_{\Omega} \rho = 0$  if  $k_{\rho} \leq k_P$ , (3.8) simplifies to

$$\partial_t \frac{1}{2} \int_{\Omega} \rho^2 \, d\mathbf{x} - \int_{\Omega} \bar{\rho} \partial_t \rho \, d\mathbf{x} = \partial_t \frac{1}{2} \int_{\Omega} \rho^2 \, d\mathbf{x},$$

which shows that squared density is conserved if  $\alpha_{\rho} = \frac{1}{2}$  and  $k_{\rho} \leq k_P$ . Next, for  $A \in \mathbb{R}$  we also have

$$\begin{aligned} \partial_t \frac{1}{2} \int_{\Omega} \rho^2 \, d\mathbf{x} - \int_{\Omega} A \partial_t \rho \, d\mathbf{x} &= (\rho_t, \rho - A) = -(\mathbf{u} \cdot \nabla (\rho - A), \rho - A) - \alpha_{\rho} ((\nabla \cdot \mathbf{u})(\rho - \bar{\rho}), \rho - A) \\ &= \left( \nabla \cdot \mathbf{u}, \frac{1}{2} (\rho - A)^2 - \alpha_{\rho} (\rho - \bar{\rho})(\rho - A) \right). \end{aligned}$$

There exists two roots of  $A$  that satisfies

$$\int_{\Omega} \frac{1}{2} (\rho - A)^2 - \alpha_{\rho} (\rho - \bar{\rho})(\rho - A) \, d\mathbf{x} = 0. \quad (3.9)$$

We only need one  $A$  to satisfy (3.9) and one of the roots are

$$\begin{aligned} A = |\Omega|^{-1} \left( \alpha_{\rho} |\Omega| \bar{\rho} + (1 - \alpha_{\rho}) \int_{\Omega} \rho \, d\mathbf{x} + \left( \alpha_{\rho}^2 |\Omega|^2 \bar{\rho}^2 - 2\alpha_{\rho}^2 |\Omega| \bar{\rho} \int_{\Omega} \rho \, d\mathbf{x} + \alpha_{\rho}^2 \left( \int_{\Omega} \rho \, d\mathbf{x} \right)^2 + 2\alpha_{\rho} |\Omega| \int_{\Omega} \rho^2 \, d\mathbf{x} \right. \right. \\ \left. \left. - 2\alpha_{\rho} \left( \int_{\Omega} \rho \, d\mathbf{x} \right)^2 - |\Omega| \int_{\Omega} \rho^2 \, d\mathbf{x} + \left( \int_{\Omega} \rho \, d\mathbf{x} \right)^2 \right)^{1/2} \right). \end{aligned}$$

This means that, if  $2k_{\rho} \leq k_P$  then there exists an  $A$  such that  $\left( \frac{1}{2} (\rho - A)^2 - \alpha_{\rho} (\rho - \bar{\rho})(\rho - A) \right) \in \mathcal{Q}$ . Because of this, we can invoke the weak divergence-free condition (3.3) to conclude that squared density is conserved.

**Kinetic energy:** Using the definition of kinetic energy, the definition of the  $L^2$ -projection (3.4) and setting  $w = \overline{\mathbf{u} \cdot \mathbf{u}}$ ,  $\mathbf{v} = \mathbf{u}$  inside the density and momentum updates (3.3) yields

$$\begin{aligned}
\frac{1}{2} \partial_t \int_{\Omega} \rho \mathbf{u} \cdot \mathbf{u} \, d\mathbf{x} &= \frac{1}{2} (\rho_t \mathbf{u}, \mathbf{u}) + (\rho \mathbf{u}_t, \mathbf{u}) = (\rho_t \mathbf{u}, \mathbf{u}) + (\rho \mathbf{u}_t, \mathbf{u}) - \frac{1}{2} (\rho_t \mathbf{u}, \mathbf{u}) \\
&= (\mathbf{m}_t, \mathbf{u}) - \frac{1}{2} (\rho_t, \mathbf{u} \cdot \mathbf{u}) = (\mathbf{m}_t, \mathbf{u}) - \frac{1}{2} (\rho_t, \overline{\mathbf{u} \cdot \mathbf{u}}) \\
&= -b(\mathbf{u}, \mathbf{m}, \mathbf{u}) - \alpha_m ((\nabla \cdot \mathbf{u}) \mathbf{m}, \mathbf{u}) - (\nabla P, \mathbf{u}) \\
&\quad - \left( \alpha_P - \frac{1}{2} \right) b(\mathbf{u}, \mathbf{m}, \mathbf{u}) - \left( \alpha_P + \frac{1}{2} \right) b(\mathbf{u}, \mathbf{u}, \mathbf{m}) - \frac{1}{2} \alpha_\rho (\nabla(\mathbf{m} \cdot \mathbf{u}), \mathbf{u}) \\
&\quad - \frac{1}{2} ((\mathbf{u} \cdot \nabla \rho, \overline{\mathbf{u} \cdot \mathbf{u}}) - \alpha_\rho (\nabla((\rho - \bar{\rho}) \overline{\mathbf{u} \cdot \mathbf{u}}), \mathbf{u})) \\
&\quad + \frac{1}{2} (\mathbf{u} \cdot \nabla \rho + \alpha_\rho (\nabla \cdot \mathbf{u})(\rho - \bar{\rho}), \overline{\mathbf{u} \cdot \mathbf{u}}).
\end{aligned}$$

Integration by parts on the pressure term and invoking the weak divergence-free constraint inside (3.3), using (2.5) on  $(\alpha_P - \frac{1}{2}) b(\mathbf{u}, \mathbf{m}, \mathbf{u})$  and integration by parts on  $\alpha_\rho (\nabla((\rho - \bar{\rho}) \overline{\mathbf{u} \cdot \mathbf{u}}), \mathbf{u})$  yields

$$\begin{aligned}
\frac{1}{2} \partial_t \int_{\Omega} \rho \mathbf{u} \cdot \mathbf{u} \, d\mathbf{x} &= -b(\mathbf{u}, \mathbf{m}, \mathbf{u}) + \left( \alpha_P - \frac{1}{2} - \alpha_m \right) ((\nabla \cdot \mathbf{u}) \mathbf{m}, \mathbf{u}) \\
&\quad + \left( \alpha_P - \frac{1}{2} \right) b(\mathbf{u}, \mathbf{u}, \mathbf{m}) - \left( \alpha_P + \frac{1}{2} \right) b(\mathbf{u}, \mathbf{u}, \mathbf{m}) - \frac{1}{2} \alpha_\rho (\nabla(\mathbf{m} \cdot \mathbf{u}), \mathbf{u}) \\
&\quad - \frac{1}{2} ((\mathbf{u} \cdot \nabla \rho, \overline{\mathbf{u} \cdot \mathbf{u}}) + \alpha_\rho ((\nabla \cdot \mathbf{u}), (\rho - \bar{\rho}) \overline{\mathbf{u} \cdot \mathbf{u}})) \\
&\quad + \frac{1}{2} (\mathbf{u} \cdot \nabla \rho + \alpha_\rho (\nabla \cdot \mathbf{u})(\rho - \bar{\rho}), \overline{\mathbf{u} \cdot \mathbf{u}}) \\
&= -b(\mathbf{u}, \mathbf{m}, \mathbf{u}) + \left( \alpha_P - \frac{1}{2} - \alpha_m \right) ((\nabla \cdot \mathbf{u}) \mathbf{m}, \mathbf{u}) \\
&\quad - b(\mathbf{u}, \mathbf{u}, \mathbf{m}) - \frac{1}{2} \alpha_\rho (\nabla(\mathbf{m} \cdot \mathbf{u}), \mathbf{u}).
\end{aligned}$$

Using (2.5) on  $b(\mathbf{u}, \mathbf{m}, \mathbf{u})$  and integration by parts on  $\frac{1}{2} \alpha_\rho (\nabla(\mathbf{m} \cdot \mathbf{u}), \mathbf{u})$  yields

$$\frac{1}{2} \partial_t \int_{\Omega} \rho \mathbf{u} \cdot \mathbf{u} \, d\mathbf{x} = \left( \alpha_P + \frac{1}{2} - \alpha_m + \frac{1}{2} \alpha_\rho \right) ((\nabla \cdot \mathbf{u}) \mathbf{m}, \mathbf{u}),$$

which means that kinetic energy is conserved if  $\alpha_m - \alpha_P - \alpha_\rho/2 = 1/2$ .

**Momentum:** We set  $\mathbf{v} = \mathbf{e}_i$  inside the momentum equations (3.3) and obtain

$$\begin{aligned}
\partial_t \int_{\Omega} \mathbf{m}_i \, d\mathbf{x} &= (\mathbf{m}_t, \mathbf{e}_i) = -b(\mathbf{u}, \mathbf{m}, \mathbf{e}_i) - \alpha_m ((\nabla \cdot \mathbf{u}) \mathbf{m}, \mathbf{e}_i) - (\nabla P, \mathbf{e}_i) \\
&\quad - \left( \alpha_P - \frac{1}{2} \right) b(\mathbf{e}_i, \mathbf{m}, \mathbf{u}) - \left( \alpha_P + \frac{1}{2} \right) b(\mathbf{e}_i, \mathbf{u}, \mathbf{m}) + \frac{1}{2} \alpha_\rho ((\nabla \cdot \mathbf{e}_i) \mathbf{m}, \mathbf{u}) \\
&\quad - \frac{1}{2} ((\mathbf{e}_i \cdot \nabla \rho, \overline{\mathbf{u} \cdot \mathbf{u}}) + \alpha_\rho ((\nabla \cdot \mathbf{e}_i)(\rho - \bar{\rho}), \overline{\mathbf{u} \cdot \mathbf{u}})) \\
&= -b(\mathbf{u}, \mathbf{m}, \mathbf{e}_i) - \alpha_m ((\nabla \cdot \mathbf{u}) \mathbf{m}, \mathbf{e}_i) - (\nabla P, \mathbf{e}_i) \\
&\quad - \left( \alpha_P - \frac{1}{2} \right) b(\mathbf{e}_i, \mathbf{m}, \mathbf{u}) - \left( \alpha_P + \frac{1}{2} \right) b(\mathbf{e}_i, \mathbf{u}, \mathbf{m}) - \frac{1}{2} (\mathbf{e}_i \cdot \nabla \rho, \overline{\mathbf{u} \cdot \mathbf{u}}),
\end{aligned}$$



since  $\mathbf{e}_i$  is a constant. Using (2.5) on  $(\alpha_P - \frac{1}{2})b(\mathbf{e}_i, \mathbf{m}, \mathbf{u})$  and  $b(\mathbf{u}, \mathbf{m}, \mathbf{e}_i)$  and integration by parts on the pressure term yield

$$\begin{aligned}
\partial_t \int_{\Omega} \mathbf{m}_i \, d\mathbf{x} &= b(\mathbf{u}, \mathbf{e}_i, \mathbf{m}) + ((\nabla \cdot \mathbf{u})\mathbf{m}, \mathbf{e}_i) - \alpha_m((\nabla \cdot \mathbf{u})\mathbf{m}, \mathbf{e}_i) + (P, \nabla \cdot \mathbf{e}_i) \\
&\quad + \left(\alpha_P - \frac{1}{2}\right)b(\mathbf{e}_i, \mathbf{u}, \mathbf{m}) - \left(\alpha_P + \frac{1}{2}\right)b(\mathbf{e}_i, \mathbf{u}, \mathbf{m}) - \frac{1}{2}(\mathbf{e}_i \cdot \nabla \rho, \overline{\mathbf{u} \cdot \mathbf{u}}) \\
&= (1 - \alpha_m)((\nabla \cdot \mathbf{u})\mathbf{m}, \mathbf{e}_i) - b(\mathbf{e}_i, \mathbf{u}, \mathbf{m}) - \frac{1}{2}(\mathbf{e}_i \cdot \nabla \rho, \overline{\mathbf{u} \cdot \mathbf{u}}) \\
&= (1 - \alpha_m)((\nabla \cdot \mathbf{u})\mathbf{m}, \mathbf{e}_i) - b(\rho \mathbf{e}_i, \mathbf{u}, \mathbf{u}) - \frac{1}{2}(\mathbf{e}_i \cdot \nabla \rho, \overline{\mathbf{u} \cdot \mathbf{u}}) \\
&= (1 - \alpha_m)((\nabla \cdot \mathbf{u})\mathbf{m}, \mathbf{e}_i) + \frac{1}{2}((\nabla \cdot (\rho \mathbf{e}_i))\mathbf{u}, \mathbf{u}) - \frac{1}{2}(\mathbf{e}_i \cdot \nabla \rho, \overline{\mathbf{u} \cdot \mathbf{u}}) \\
&= (1 - \alpha_m)((\nabla \cdot \mathbf{u})\mathbf{m}, \mathbf{e}_i),
\end{aligned}$$

where (2.6) was used in the third equality and (2.4) was used in the second equality and (3.4) in the last step. Thus, momentum is conserved if  $\alpha_m = 1$ .

**Angular momentum:** Conservation of angular momentum is derived by setting  $\mathbf{v} = \phi_i$  inside (3.3) to obtain

$$\begin{aligned}
\partial_t \int_{\Omega} (\mathbf{m} \times \mathbf{x})_i \, d\mathbf{x} &= (\mathbf{m}_t, \phi_i) = -b(\mathbf{u}, \mathbf{m}, \phi_i) - \alpha_m((\nabla \cdot \mathbf{u})\mathbf{m}, \phi_i) - (\nabla P, \phi_i) \\
&\quad - \left(\alpha_P - \frac{1}{2}\right)b(\phi_i, \mathbf{m}, \mathbf{u}) - \left(\alpha_P + \frac{1}{2}\right)b(\phi_i, \mathbf{u}, \mathbf{m}) + \frac{1}{2}\alpha_\rho((\nabla \cdot \phi_i)\mathbf{m}, \mathbf{u}) \\
&\quad - \frac{1}{2}((\phi_i \cdot \nabla \rho, \overline{\mathbf{u} \cdot \mathbf{u}}) + \alpha_\rho((\nabla \cdot \phi_i)(\rho - \bar{\rho}), \overline{\mathbf{u} \cdot \mathbf{u}})) \\
&= -b(\mathbf{u}, \mathbf{m}, \phi_i) - \alpha_m((\nabla \cdot \mathbf{u})\mathbf{m}, \phi_i) - (\nabla P, \phi_i) \\
&\quad - \left(\alpha_P - \frac{1}{2}\right)b(\phi_i, \mathbf{m}, \mathbf{u}) - \left(\alpha_P + \frac{1}{2}\right)b(\phi_i, \mathbf{u}, \mathbf{m}) - \frac{1}{2}(\phi_i \cdot \nabla \rho, \overline{\mathbf{u} \cdot \mathbf{u}}),
\end{aligned}$$

since  $\nabla \cdot \phi_i = 0$ . Using (2.5) on  $(\alpha_P - \frac{1}{2})b(\phi_i, \mathbf{m}, \mathbf{u})$  and  $b(\mathbf{u}, \mathbf{m}, \phi_i)$  and integration by parts on the pressure term yield

$$\begin{aligned}
\partial_t \int_{\Omega} (\mathbf{m} \times \mathbf{x})_i \, d\mathbf{x} &= b(\mathbf{u}, \phi_i, \mathbf{m}) + ((\nabla \cdot \mathbf{u})\mathbf{m}, \phi_i) - \alpha_m((\nabla \cdot \mathbf{u})\mathbf{m}, \phi_i) + (P, \nabla \cdot \phi_i) \\
&\quad + \left(\alpha_P - \frac{1}{2}\right)b(\phi_i, \mathbf{u}, \mathbf{m}) - \left(\alpha_P + \frac{1}{2}\right)b(\phi_i, \mathbf{u}, \mathbf{m}) - \frac{1}{2}(\phi_i \cdot \nabla \rho, \overline{\mathbf{u} \cdot \mathbf{u}}) \\
&= b(\mathbf{u}, \phi_i, \mathbf{m}) + (1 - \alpha_m)((\nabla \cdot \mathbf{u})\mathbf{m}, \phi_i) - b(\phi_i, \mathbf{u}, \mathbf{m}) - \frac{1}{2}(\phi_i \cdot \nabla \rho, \overline{\mathbf{u} \cdot \mathbf{u}}) \\
&= b(\mathbf{u}, \phi_i, \mathbf{m}) + (1 - \alpha_m)((\nabla \cdot \mathbf{u})\mathbf{m}, \phi_i) - b(\rho \phi_i, \mathbf{u}, \mathbf{u}) - \frac{1}{2}(\phi_i \cdot \nabla \rho, \overline{\mathbf{u} \cdot \mathbf{u}}) \\
&= b(\mathbf{u}, \phi_i, \mathbf{m}) + (1 - \alpha_m)((\nabla \cdot \mathbf{u})\mathbf{m}, \phi_i) + \frac{1}{2}((\nabla \cdot (\rho \phi_i))\mathbf{u}, \mathbf{u}) - \frac{1}{2}(\phi_i \cdot \nabla \rho, \overline{\mathbf{u} \cdot \mathbf{u}}) \\
&= b(\mathbf{u}, \phi_i, \mathbf{m}) + (1 - \alpha_m)((\nabla \cdot \mathbf{u})\mathbf{m}, \phi_i),
\end{aligned}$$

where (2.6) was used in the third equality, (2.4) was used in the second equality and (3.4) in the last step. Next, by using (2.2) it can be shown that

$$\begin{aligned}
b(\mathbf{u}, \phi_i, \mathbf{m}) &= b(\mathbf{u}, \phi_i, \mathbf{u}\rho) = \frac{1}{2}b(\mathbf{u}, \phi_i, \mathbf{u}\rho) + \frac{1}{2}b(\mathbf{u}, \phi_i, \mathbf{u}\rho) \\
&= \frac{1}{2}((\nabla \phi_i)^\top \mathbf{u}, \mathbf{u}\rho) + \frac{1}{2}((\nabla \phi_i)^\top \mathbf{u}, \mathbf{u}\rho) = \frac{1}{2}((\nabla \phi_i)^\top \mathbf{u}, \mathbf{u}\rho) + \frac{1}{2}((\nabla \phi_i)^\top \mathbf{u}, \mathbf{u}\rho) = 0,
\end{aligned}$$

since  $\nabla\phi_i + (\nabla\phi_i)^\top = 0$ . Since  $b(\mathbf{u}, \phi_i, \mathbf{m}) = 0$ , angular momentum is conserved if  $\alpha_{\mathbf{m}} = 1$ .  $\square$

#### 4. Properties of viscous regularizations.

In this section, we investigate how viscous regularizations of the incompressible Euler equations (2.1) affect conservation properties. We note that the purpose of this section is to investigate the properties of the model and not to investigate the properties of the numerical method. To simplify the analysis we assume that  $\nabla \cdot \mathbf{u} = 0$  holds pointwise and assume periodic boundary conditions. We consider a viscous regularization of the following form

$$\begin{aligned} \partial_t \rho + \mathbf{u} \cdot \nabla \rho &= \nabla \cdot \mathbf{f}_\rho, \\ \partial_t \mathbf{m} + \mathbf{u} \cdot \nabla \mathbf{m} + \nabla p &= \mathbf{f} + \nabla \cdot (\mu (\nabla \mathbf{u} + (\nabla \mathbf{u})^\top)) + \mathbf{f}_m, \quad (\mathbf{x}, t) \in \Omega \times (0, T], \\ \nabla \cdot \mathbf{u} &= 0, \\ \mathbf{u}(\mathbf{x}, 0) &= \mathbf{u}_0(\mathbf{x}), \\ \rho(\mathbf{x}, 0) &= \rho_0(\mathbf{x}), \quad \mathbf{x} \in \Omega, \end{aligned} \tag{4.1}$$

where  $\mu \geq 0$  is the dynamic viscosity coefficient which in general is space-dependent,  $\mathbf{f}_\rho := \kappa \nabla \rho$ , where  $\kappa \geq 0$  is a mass diffusivity coefficient which also is space-dependent. In this work, we define  $\mathbf{f}_m$  as

$$\mathbf{f}_m(\mathbf{u}, \mathbf{f}_\rho) := A_1(\nabla \mathbf{f}_\rho) \mathbf{u} + A_2(\nabla \mathbf{f}_\rho)^\top \mathbf{u} + A_3(\nabla \mathbf{u}) \mathbf{f}_\rho + A_4(\nabla \mathbf{u})^\top \mathbf{f}_\rho + A_5(\nabla \cdot \mathbf{f}_\rho) \mathbf{u}, \tag{4.2}$$

where  $A_i \in \mathbb{R}$ . Depending on how the constants  $A_i$  are chosen, different properties of the model are obtained and this is summarized in Theorem 4.1.

**Theorem 4.1.** *If  $\mathbf{f} = 0$ , the system (4.1):*

1. *Dissipates kinetic energy if  $A_1 + A_2 - A_3 = 0$  and  $A_5 - \frac{1}{2}A_4 = \frac{1}{2}$ .*
2. *Conserves momentum if  $A_1 - A_3 = 0$  and  $A_5 - A_4 = 0$ .*
3. *Conserves angular momentum if  $A_1 - A_3 = 0$  and  $A_5 - A_4 = 0$  and  $A_2 = A_4$ .*

*Proof.* We divide the proof into several sections. Extending the proofs to other boundary conditions such as no-slip ( $\mathbf{u} = 0|_{\partial\Omega}$ ) can be done by using the proof technique in [5, Sec 3.1.2] or [16, Sec 3.1.2].

**Kinetic energy:** Repeating similar steps on (4.1) as in the proof of Theorem 3.1 and assuming  $\nabla \cdot \mathbf{u} = 0$  yields

$$\frac{1}{2} \partial_t \int_{\Omega} \rho \mathbf{u} \cdot \mathbf{u} \, d\mathbf{x} = (\mathbf{m}_t, \mathbf{u}) - \frac{1}{2} (\rho_t, \mathbf{u} \cdot \mathbf{u}) = (\mathbf{f}_m, \mathbf{u}) - \frac{1}{2} ((\nabla \cdot \mathbf{f}_\rho) \mathbf{u}, \mathbf{u}) + (\nabla \cdot (\mu (\nabla \mathbf{u} + (\nabla \mathbf{u})^\top)), \mathbf{u}),$$

where only the viscous terms determine if kinetic energy is dissipated. Next, we obtain

$$\begin{aligned} \frac{1}{2} \partial_t \int_{\Omega} \rho \mathbf{u} \cdot \mathbf{u} \, d\mathbf{x} &= A_1 b(\mathbf{u}, \mathbf{f}_\rho, \mathbf{u}) + A_2 b(\mathbf{u}, \mathbf{f}_\rho, \mathbf{u}) + A_3 b(\mathbf{u}, \mathbf{u}, \mathbf{f}_\rho) + A_4 b(\mathbf{f}_\rho, \mathbf{u}, \mathbf{u}) \\ &\quad + A_5 ((\nabla \cdot \mathbf{f}_\rho) \mathbf{u}, \mathbf{u}) - \frac{1}{2} ((\nabla \cdot \mathbf{f}_\rho) \mathbf{u}, \mathbf{u}) + (\nabla \cdot (\mu (\nabla \mathbf{u} + (\nabla \mathbf{u})^\top)), \mathbf{u}), \\ &= A_1 b(\mathbf{u}, \mathbf{f}_\rho, \mathbf{u}) + A_2 b(\mathbf{u}, \mathbf{f}_\rho, \mathbf{u}) - A_3 b(\mathbf{u}, \mathbf{f}_\rho, \mathbf{u}) - \frac{1}{2} A_4 ((\nabla \cdot \mathbf{f}_\rho) \mathbf{u}, \mathbf{u}) \\ &\quad + A_5 ((\nabla \cdot \mathbf{f}_\rho) \mathbf{u}, \mathbf{u}) - \frac{1}{2} ((\nabla \cdot \mathbf{f}_\rho) \mathbf{u}, \mathbf{u}) - (\mu (\nabla \mathbf{u} + (\nabla \mathbf{u})^\top), \nabla \mathbf{u}), \end{aligned} \tag{4.3}$$

by using integration by parts on the  $\mu$  term and using (2.5) on the  $A_3$  term and (2.6) on the  $A_4$  term. Using that the contraction between a symmetric and anti-symmetric matrix with zero diagonal is zero [18, Ch 11.2.1], i.e.,  $(A + A^\top) : (A - A^\top) = 0$  where  $A$  is a square matrix, one can show that

$$\begin{aligned} \left( \mu \left( \nabla \mathbf{u} + (\nabla \mathbf{u})^\top \right), \nabla \mathbf{u} \right) &= \frac{1}{2} \left( \mu \left( \nabla \mathbf{u} + (\nabla \mathbf{u})^\top \right), \nabla \mathbf{u} + (\nabla \mathbf{u})^\top \right) \\ &\quad + \frac{1}{2} \left( \mu \left( \nabla \mathbf{u} + (\nabla \mathbf{u})^\top \right), \nabla \mathbf{u} - (\nabla \mathbf{u})^\top \right) \\ &= \frac{1}{2} \left( \mu \left( \nabla \mathbf{u} + (\nabla \mathbf{u})^\top \right), \nabla \mathbf{u} + (\nabla \mathbf{u})^\top \right). \end{aligned} \quad (4.4)$$

Inserting (4.4) into (4.3) gives

$$\begin{aligned} \frac{1}{2} \partial_t \int_{\Omega} \rho \mathbf{u} \cdot \mathbf{u} \, d\mathbf{x} &= A_1 b(\mathbf{u}, \mathbf{f}_\rho, \mathbf{u}) + A_2 b(\mathbf{u}, \mathbf{f}_\rho, \mathbf{u}) - A_3 b(\mathbf{u}, \mathbf{f}_\rho, \mathbf{u}) - \frac{1}{2} A_4 ((\nabla \cdot \mathbf{f}_\rho) \mathbf{u}, \mathbf{u}) \\ &\quad + A_5 ((\nabla \cdot \mathbf{f}_\rho) \mathbf{u}, \mathbf{u}) - \frac{1}{2} ((\nabla \cdot \mathbf{f}_\rho) \mathbf{u}, \mathbf{u}) - \frac{1}{2} \|\sqrt{\mu} (\nabla \mathbf{u} + (\nabla \mathbf{u})^\top)\|^2. \end{aligned} \quad (4.5)$$

From (4.5), the conditions necessary for kinetic energy to be dissipated are

$$A_1 + A_2 - A_3 = 0 \text{ and } A_5 - \frac{1}{2} A_4 = \frac{1}{2}.$$

**Momentum:** Repeating similar steps on (4.1) as in the proof of Theorem 3.1 and assuming  $\nabla \cdot \mathbf{u} = 0$  yields

$$\partial_t \int_{\Omega} \mathbf{m}_i \, d\mathbf{x} = (\mathbf{m}_t, \mathbf{e}_i) = (\nabla \cdot (\mu (\nabla \mathbf{u} + (\nabla \mathbf{u})^\top)), \mathbf{e}_i) + (\mathbf{f}_m, \mathbf{e}_i),$$

where only the viscous terms determine if momentum is conserved. Performing integration by parts on the  $\mu$  term yields

$$\partial_t \int_{\Omega} \mathbf{m}_i \, d\mathbf{x} = A_1 b(\mathbf{e}_i, \mathbf{f}_\rho, \mathbf{u}) + A_2 b(\mathbf{u}, \mathbf{f}_\rho, \mathbf{e}_i) + A_3 b(\mathbf{e}_i, \mathbf{u}, \mathbf{f}_\rho) + A_4 b(\mathbf{f}_\rho, \mathbf{u}, \mathbf{e}_i) + A_5 ((\nabla \cdot \mathbf{f}_\rho) \mathbf{u}, \mathbf{e}_i). \quad (4.6)$$

Using (2.5) on the  $A_3$ ,  $A_2$  and  $A_4$  terms inside (4.6) gives

$$\partial_t \int_{\Omega} \mathbf{m}_i \, d\mathbf{x} = A_1 b(\mathbf{e}_i, \mathbf{f}_\rho, \mathbf{u}) - A_3 b(\mathbf{e}_i, \mathbf{f}_\rho, \mathbf{u}) - A_4 ((\nabla \cdot \mathbf{f}_\rho) \mathbf{u}, \mathbf{e}_i) + A_5 ((\nabla \cdot \mathbf{f}_\rho) \mathbf{u}, \mathbf{e}_i),$$

which leads to the conditions necessary for momentum to be conserved

$$A_1 - A_3 = 0 \text{ and } A_5 - A_4 = 0.$$

**Angular momentum:** Repeating similar steps on (4.1) as in the proof of Theorem 3.1 and assuming  $\nabla \cdot \mathbf{u} = 0$  yields

$$\partial_t \int_{\Omega} (\mathbf{m} \times \mathbf{x})_i \, d\mathbf{x} = (\nabla \cdot (\mu (\nabla \mathbf{u} + (\nabla \mathbf{u})^\top)), \phi_i) + (\mathbf{f}_m, \phi_i).$$

Performing integration by parts on the  $\mu$  term yields

$$\partial_t \int_{\Omega} (\mathbf{m} \times \mathbf{x})_i \, d\mathbf{x} = -(\mu (\nabla \mathbf{u} + (\nabla \mathbf{u})^\top), \nabla \phi_i) + (\mathbf{f}_m, \phi_i).$$

Next, using that the contraction between a symmetric and anti-symmetric matrix with zero diagonal is zero [18, Ch 11.2.1], one can show that

$$\begin{aligned} (\mu (\nabla \mathbf{u} + (\nabla \mathbf{u})^\top), \nabla \phi_i) &= \left( \frac{1}{2} \mu (\nabla \mathbf{u} + (\nabla \mathbf{u})^\top), \nabla \phi_i + (\nabla \phi_i)^\top \right) \\ &\quad + \left( \frac{1}{2} \mu (\nabla \mathbf{u} + (\nabla \mathbf{u})^\top), \nabla \phi_i - (\nabla \phi_i)^\top \right) \\ &= \left( \frac{1}{2} \mu (\nabla \mathbf{u} + (\nabla \mathbf{u})^\top), \nabla \phi_i + (\nabla \phi_i)^\top \right). \end{aligned}$$

Since  $\nabla \phi_i = -\nabla \phi_i^\top$  we are left with

$$\begin{aligned} \partial_t \int_{\Omega} (\mathbf{m} \times \mathbf{x})_i \, d\mathbf{x} &= (\mathbf{f}_m, \phi_i) = A_1 b(\phi_i, \mathbf{f}_\rho, \mathbf{u}) + A_2 b(\mathbf{u}, \mathbf{f}_\rho, \phi_i) \\ &\quad + A_3 b(\phi_i, \mathbf{u}, \mathbf{f}_\rho) + A_4 b(\mathbf{f}_\rho, \mathbf{u}, \phi_i) + A_5 ((\nabla \cdot \mathbf{f}_\rho) \mathbf{u}, \phi_i). \end{aligned}$$

Using (2.5) on the  $A_3$ ,  $A_2$  and  $A_4$  terms and using that  $\nabla \cdot \mathbf{u} = \nabla \cdot \phi_i = 0$  gives

$$\begin{aligned} \partial_t \int_{\Omega} (\mathbf{m} \times \mathbf{x})_i \, d\mathbf{x} &= A_1 b(\phi_i, \mathbf{f}_\rho, \mathbf{u}) - A_2 b(\mathbf{u}, \phi_i, \mathbf{f}_\rho) - A_3 b(\phi_i, \mathbf{f}_\rho, \mathbf{u}) \\ &\quad - A_4 b(\mathbf{f}_\rho, \phi_i, \mathbf{u}) - A_4 ((\nabla \cdot \mathbf{f}_\rho) \mathbf{u}, \phi_i) + A_5 ((\nabla \cdot \mathbf{f}_\rho) \mathbf{u}, \phi_i). \end{aligned}$$

Next, using the definition of the trilinear form (2.2) yields

$$\begin{aligned} \partial_t \int_{\Omega} (\mathbf{m} \times \mathbf{x})_i \, d\mathbf{x} &= A_1 b(\phi_i, \mathbf{f}_\rho, \mathbf{u}) - A_2 ((\nabla \phi_i)^\top \mathbf{u}, \mathbf{f}_\rho) - A_3 b(\phi_i, \mathbf{f}_\rho, \mathbf{u}) \\ &\quad - A_4 ((\nabla \phi_i) \mathbf{u}, \mathbf{f}_\rho) - A_4 ((\nabla \cdot \mathbf{f}_\rho) \mathbf{u}, \phi_i) + A_5 ((\nabla \cdot \mathbf{f}_\rho) \mathbf{u}, \phi_i), \end{aligned}$$

which leads to the conditions necessary for angular momentum to be conserved

$$A_1 - A_3 = 0 \text{ and } A_5 - A_4 = 0 \text{ and } A_2 = A_4,$$

since  $\nabla \phi_i + (\nabla \phi_i)^\top = 0$ .

□

#### 4.1. Discussion.

One implication of Theorem 4.1 is that there is no viscous regularization ( $\kappa > 0$ ) that simultaneously dissipates kinetic energy and conserves angular momentum. Another implication is that a unique viscous regularization dissipates kinetic energy and conserves momentum. This can be seen by combining the kinetic energy and the momentum conditions in Theorem 4.1 to arrive at  $A_5 = A_4 = 1$ ,  $A_2 = 0$  and  $A_1 = A_3$ . Setting these conditions inside (4.2) and performing some simplifications lead to the following viscous flux

$$\mathbf{f}_{GP} := (\nabla \mathbf{u})^\top \mathbf{f}_\rho + (\nabla \cdot \mathbf{f}_\rho) \mathbf{u} + A_1 (\nabla \mathbf{f}_\rho) \mathbf{u} + A_1 (\nabla \mathbf{u}) \mathbf{f}_\rho = \nabla \cdot (\mathbf{f}_\rho \otimes \mathbf{u}) + A_1 \nabla (\mathbf{f}_\rho \cdot \mathbf{u}), \quad (4.7)$$

where the second term does not change the model since it only results that a modified pressure is solved for, i.e.,  $P = p - A_1 \mathbf{f}_\rho \cdot \mathbf{u}$ , and does not affect the behavior of density and velocity. Since that term is not important, we are left with the so-called Guermond-Popov viscous flux [12]. Compared to (4.7), the Guermond-Popov flux [12] is simplified since it now is in the incompressible setting instead of the compressible setting. This means that, if we only consider the density and momentum contribution of [12], it is exactly the same as (4.7) and (4.1).

Combining the last two conditions of Theorem 4.1 leads to a family of viscous regularizations that conserve momentum and angular momentum. Below two examples of these are given

$$\begin{aligned} \mathbf{f}_0 &:= 0, \\ \mathbf{f}_{KS} &:= \nabla \cdot (\mathbf{f}_\rho \otimes \mathbf{u} + \mathbf{u} \otimes \mathbf{f}_\rho), \end{aligned} \quad (4.8)$$

where  $\mathbf{f}_0$  has previously been used in the variable density flow literature [3]. From Ficks law, Kažihov and Smagulov [17] derived and proposed (4.8). They showed kinetic energy dissipation assuming that  $\kappa$  is constant and

$$\kappa < \frac{2\mu}{\max_{\Omega} \rho - \min_{\Omega} \rho}. \quad (4.9)$$

It is not clear if (4.9) is true for all fluid pairs at all temperatures. For example, consider hydrogen gas  $\text{H}_2$  and sulfur hexafluoride gas  $\text{SF}_6$  at room temperature. Values of dynamic viscosity, density and pair-wise mass diffusivity are given in Table 3. Inserting these values into (4.9) shows an order of magnitude violation:

$$\begin{aligned} \frac{2\mu}{\max_{\Omega} \rho - \min_{\Omega} \rho} &= \frac{2 \cdot 15.3 \cdot 10^{-6}}{6.07 - 0.0838} \text{ [m}^2\text{/sec]} \\ &= 5.1 \cdot 10^{-6} \text{ [m}^2\text{/sec]}, \end{aligned}$$

$$\kappa = 4.12 \cdot 10^{-5} \text{ [m}^2\text{/sec]} \not\leq 5.1 \cdot 10^{-6} \text{ [m}^2\text{/sec]}.$$

Table 3: Experimental values from [15] of dynamic viscosity at 300 K, 1 kPa and pair-wise mass diffusion at 20 °C, 1 atm. Density from ideal gas law.

|               | $\mu$ [Pa · sec]     | $\rho$ [kg/m <sup>3</sup> ] | $\kappa$ [m <sup>2</sup> /sec] |
|---------------|----------------------|-----------------------------|--------------------------------|
| $\text{H}_2$  | $8.9 \cdot 10^{-6}$  | 0.0838                      | $4.12 \cdot 10^{-5}$           |
| $\text{SF}_6$ | $15.3 \cdot 10^{-6}$ | 6.07                        | $4.12 \cdot 10^{-5}$           |

## 5. Fully discrete conservative method.

In this section, we describe the fully discrete method approximating the incompressible Navier-Stokes equations (4.1). Let  $(\rho^n, \mathbf{u}^n, P^n) \in (\mathcal{M}, \mathcal{V}, \mathcal{Q})$  be solutions at time  $t_n$ , where the time-levels are defined as  $0 = t_0 < t_1 < \dots < t_{N_t} = T$  and  $N_t$  denotes the total number of time-levels. Let  $\Delta t_{n+j} := t_{n+j+1} - t_{n+j}$  denote the time step. We also define  $\mathbf{u}^{n+1/2} := \frac{\mathbf{u}^n + \mathbf{u}^{n+1}}{2}$ .

We propose using the second-order accurate time-stepping method based on the modified Crank-Nicolson method by Gawlik and Gay-Balmaz [8] which has favorable fully discrete properties. Applying this method on (3.3) yields: Given  $(\rho^n, \mathbf{u}^n)$ , find  $(\rho^{n+1}, \mathbf{u}^{n+1}, P^{n+1/2}) \in (\mathcal{M}, \mathcal{V}, \mathcal{Q})$  such that

$$\begin{aligned}
& \left( \frac{\rho^{n+1} - \rho^n}{\Delta t_n} + \mathbf{u}^{n+1/2} \cdot \nabla \rho^{n+1/2} + \alpha_\rho \left( \nabla \cdot \mathbf{u}^{n+1/2} \right) \left( \rho^{n+1/2} - \bar{\rho}^{n+1/2} \right), w \right) \\
& \quad + \left( \kappa \nabla \rho^{n+1/2}, \nabla w \right) = 0, \quad \forall w \in \mathcal{M}, \\
& \quad \left( \frac{\mathbf{m}^{n+1} - \mathbf{m}^n}{\Delta t_n}, \mathbf{v} \right) + b \left( \mathbf{u}^{n+1/2}, \mathbf{m}^{n+1/2}, \mathbf{v} \right) \\
& \quad + \alpha_m \left( \left( \nabla \cdot \mathbf{u}^{n+1/2} \right) \mathbf{m}^{n+1/2}, \mathbf{v} \right) + \left( \nabla P^{n+1/2}, \mathbf{v} \right) \\
& \quad + \left( \alpha_P - \frac{1}{2} \right) b \left( \mathbf{v}, \mathbf{m}^{n+1/2}, \mathbf{u}^{n+1/2} \right) \\
& \quad + \left( \alpha_P + \frac{1}{2} \right) b \left( \mathbf{v}, \mathbf{u}^{n+1/2}, \mathbf{m}^{n+1/2} \right) + \frac{\alpha_\rho}{2} \left( \nabla \left( \mathbf{m}^{n+1/2} \cdot \mathbf{u}^{n+1/2} \right), \mathbf{v} \right) \\
& \quad + \frac{1}{2} \left( \left( \mathbf{v} \cdot \nabla \rho^{n+1/2}, \overline{\mathbf{u}^n \cdot \mathbf{u}^{n+1}} \right) - \alpha_\rho \left( \nabla \left( \left( \rho^{n+1/2} - \bar{\rho}^{n+1/2} \right) \overline{\mathbf{u}^n \cdot \mathbf{u}^{n+1}} \right), \mathbf{v} \right) \right) \\
& \quad + \left( \mu \left( \nabla \mathbf{u}^{n+1/2} + \left( \nabla \mathbf{u}^{n+1/2} \right)^\top \right), \nabla \mathbf{v} \right) \\
& \quad - \left( \mathbf{f}^{n+1/2}, \mathbf{v} \right) - \left( \mathbf{f}_m \left( \mathbf{u}^{n+1/2}, \mathbf{f}_\rho^{n+1/2} \right), \mathbf{v} \right) = 0, \quad \forall \mathbf{v} \in \mathcal{V}, \\
& \quad \left( \nabla \cdot \mathbf{u}^{n+1/2}, q \right) = 0, \quad \forall q \in \mathcal{Q}.
\end{aligned} \tag{5.1}$$

Note that the term  $\overline{\mathbf{u} \cdot \mathbf{u}}$  has been discretized as  $\overline{\mathbf{u}^n \cdot \mathbf{u}^{n+1}}$  which is different from the usual Crank-Nicolson method.

### 5.0.1. Properties of the fully discrete method.

This section is a fully discrete analog of Section 3.2 and aims to verify that the fully discrete method satisfies the properties of Table 1. Provided that the conditions of Table 1 are fulfilled, all of the properties are retained at the fully discrete level except conservation of momentum and angular momentum. To conserve momentum and angular momentum, the term  $\overline{\mathbf{u}^n \cdot \mathbf{u}^{n+1}}$  should be discretized as  $\overline{\mathbf{u}^{n+1/2} \cdot \mathbf{u}^{n+1/2}}$  instead but this will lead to a loss of conservation of kinetic energy. Additional techniques are required to conserve both kinetic energy and momentum and angular momentum. For example, recently Zhang et al. [29] used the so-called scalar auxiliary variable (SAV) technique to enhance their time-stepping scheme to be able to conserve both kinetic energy and momentum.

**Proposition 5.1.** *The properties of Table 1, except momentum and angular momentum, hold at the fully discrete level for (5.1) provided that the conditions inside the table are fulfilled.*

**Mass:** Repeating the steps of the proof of Theorem 3.1 on (5.1) yields

$$\int_{\Omega} \rho^{n+1} \, d\mathbf{x} = \int_{\Omega} \rho^n \, d\mathbf{x} + \Delta t_n (1 - \alpha_\rho) \left( \nabla \cdot \mathbf{u}^{n+1/2}, \rho^{n+1/2} - \bar{\rho}^{n+1/2} \right),$$

and similar steps can be performed to show that  $(\rho^{n+1/2} - \bar{\rho}^{n+1/2}) \in \mathcal{Q}$  provided that  $k_\rho \leq k_P$ . Mass is conserved if  $k_\rho \leq k_P$  or if  $\alpha_\rho = 1$ .

**Squared density:** Setting  $w = \rho^{n+1/2} - \bar{\rho}^{n+1/2}$  inside (5.1) and repeating the steps of the proof of Theorem 3.1 yields

$$\left( \rho^{n+1} - \rho^n, \rho^{n+1/2} - \bar{\rho}^{n+1/2} \right) = \Delta t_n \left( \frac{1}{2} - \alpha_\rho \right) \left( \left( \nabla \cdot \mathbf{u}^{n+1/2} \right) \left( \rho^{n+1/2} - \bar{\rho}^{n+1/2} \right), \rho^{n+1/2} - \bar{\rho}^{n+1/2} \right).$$

Simplifying the left-hand side finally yields

$$\begin{aligned} \frac{1}{2}\|\rho^{n+1}\|^2 - (\rho^{n+1}, \bar{\rho}^{n+1/2}) &= \frac{1}{2}\|\rho^n\|^2 - (\rho^n, \bar{\rho}^{n+1/2}) \\ &+ \Delta t_n \left( \frac{1}{2} - \alpha_\rho \right) \left( (\nabla \cdot \mathbf{u}^{n+1/2}) (\rho^{n+1/2} - \bar{\rho}^{n+1/2}), \rho^{n+1/2} - \bar{\rho}^{n+1/2} \right), \end{aligned}$$

which is a fully discrete equivalent of (3.7). If  $\bar{\rho}^{n+1/2} = \frac{1}{|\Omega|} \int_\Omega \rho^{n+1/2} d\mathbf{x}$  then

$$\frac{1}{2}\|\rho^{n+1}\|^2 - (\rho^{n+1}, \bar{\rho}^{n+1/2}) - \left( \frac{1}{2}\|\rho^n\|^2 - (\rho^n, \bar{\rho}^{n+1/2}) \right),$$

simplifies to

$$\frac{1}{2} \left( \|\rho^{n+1}\|^2 - \left( \int_\Omega \rho^{n+1} d\mathbf{x} \right)^2 \right) - \frac{1}{2} \left( \|\rho^n\|^2 - \left( \int_\Omega \rho^n d\mathbf{x} \right)^2 \right),$$

which is a fully discrete equivalent of (3.8).

Lastly, similar steps can be performed to show that for  $A \in \mathbb{R}$

$$\begin{aligned} \frac{1}{2}\|\rho^{n+1}\|^2 - (\rho^{n+1}, A) &= \frac{1}{2}\|\rho^n\|^2 - (\rho^n, A) \\ &+ \Delta t_n \left( \nabla \cdot \mathbf{u}^{n+1/2}, \frac{1}{2} (\rho^{n+1/2} - A)^2 - \alpha_\rho (\rho^{n+1/2} - \bar{\rho}^{n+1/2}) (\rho^{n+1/2} - A) \right). \end{aligned}$$

There exists an  $A$  such that  $\left( \frac{1}{2} (\rho^{n+1/2} - A)^2 - \alpha_\rho (\rho^{n+1/2} - \bar{\rho}^{n+1/2}) (\rho^{n+1/2} - A) \right) \in \mathcal{Q}$  provided that  $2k_\rho \leq k_P$ . This means that squared density is conserved if  $2k_\rho \leq k_P$  by using the weak divergence-free condition (5.1) and that mass is conserved.

**Shift invariance:** Substituting  $\rho^{n+j}$  with  $\rho^{n+j} + c$  and repeating the steps of the proof of Theorem 3.1 shows that the density update (5.1) is invariant if  $\alpha_\rho = 0$  or if  $\bar{\rho}^{n+1/2} = \frac{1}{|\Omega|} \int_\Omega \rho^{n+1/2} d\mathbf{x}$ .

**Kinetic energy:** We begin by using the identity from [8, Sec 3] and the definition of the  $L^2$  projection (3.4) to obtain

$$\begin{aligned} \frac{1}{2}\|\sqrt{\rho^{n+1}}\mathbf{u}^{n+1}\|^2 - \frac{1}{2}\|\sqrt{\rho^n}\mathbf{u}^n\|^2 &= (\rho^{n+1}\mathbf{u}^{n+1} - \rho^n\mathbf{u}^n, \mathbf{u}^{n+1/2}) - \frac{1}{2}(\rho^{n+1} - \rho^n, \mathbf{u}^n \cdot \mathbf{u}^{n+1}) \\ &= (\rho^{n+1}\mathbf{u}^{n+1} - \rho^n\mathbf{u}^n, \mathbf{u}^{n+1/2}) - \frac{1}{2}(\rho^{n+1} - \rho^n, \overline{\mathbf{u}^n \cdot \mathbf{u}^{n+1}}). \end{aligned}$$

Next, repeating the steps of the proof of Theorem 3.1 on (5.1) leads to

$$\frac{1}{2} \left( \|\sqrt{\rho^{n+1}}\mathbf{u}^{n+1}\|^2 - \|\sqrt{\rho^n}\mathbf{u}^n\|^2 \right) = \Delta t_n \left( \alpha_m - \frac{1}{2}\alpha_\rho - \frac{1}{2} - \alpha_P \right) \left( (\nabla \cdot \mathbf{u}^{n+1/2}) \mathbf{m}^{n+1/2}, \mathbf{u}^{n+1/2} \right),$$

which shows that kinetic energy is conserved if  $\alpha_m - \alpha_P - \alpha_\rho/2 = 1/2$ .

**Momentum:** Setting  $\mathbf{v} = \mathbf{e}_i$  inside (5.1) and repeating the steps of the proof of Theorem 3.1 yields

$$\begin{aligned} \int_\Omega \mathbf{m}_i^{n+1} d\mathbf{x} &= \int_\Omega \mathbf{m}_i^n d\mathbf{x} + (1 - \alpha_m) \left( (\nabla \cdot \mathbf{u}^{n+1/2}) \mathbf{m}^{n+1/2}, \mathbf{e}_i \right) \\ &+ \frac{1}{2} \left( \mathbf{e}_i \cdot \nabla \rho^{n+1/2}, \mathbf{u}^{n+1/2} \cdot \mathbf{u}^{n+1/2} - \mathbf{u}^n \cdot \mathbf{u}^{n+1} \right). \end{aligned} \tag{5.2}$$

This means that momentum is not conserved due to the last term in (5.2).

**Angular momentum:** Setting  $\mathbf{v} = \phi_i$  inside (5.1) and repeating the steps of the proof of Theorem 3.1 yields

$$\int_{\Omega} (\mathbf{m} \times \mathbf{x})_i^{n+1} d\mathbf{x} = \int_{\Omega} (\mathbf{m} \times \mathbf{x})_i^n d\mathbf{x} + (1 - \alpha_m) \left( (\nabla \cdot \mathbf{u}^{n+1/2}) \mathbf{m}^{n+1/2}, \phi_i \right) + \frac{1}{2} \left( \phi_i \cdot \nabla \rho^{n+1/2}, \mathbf{u}^{n+1/2} \cdot \mathbf{u}^{n+1/2} - \mathbf{u}^n \cdot \mathbf{u}^{n+1} \right). \quad (5.3)$$

This means that angular momentum is not conserved due to the last term in (5.3).

### 5.1. Adaptive time-stepping

We use a simple adaptive time-stepping algorithm based on the CFL condition. Given user-defined parameters  $s_{\min}$  and  $s_{\max}$ , the next time step is computed using the following adaptive algorithm:

---

**Algorithm 1** A simplified version of the time step control algorithm from [11, Sec 5.4] used to compute the next time step  $\Delta t_n$  given user-defined parameters  $s_{\max}, s_{\min}$ .

---

```

/* Compute time step increment based on CFL condition */
s_cfl = CFL min_{x in Omega} h(x) / (||u^n||_{l2} Delta t_{n-1})
/* Make sure the next time step t_n is bounded by s_max t_{n-1} */
s = min(s_cfl, s_max)
Delta t_n = s Delta t_{n-1}
if s < s_min then
  | Repeat previous time step with Delta t_n instead
end
return Time step Delta t_n and flag whether to repeat the time step or not

```

---

## 6. Numerical validation.

The goal of this section is to numerically compare the formulations from Table 2. The table includes newly developed formulations and formulations previously known from the literature. Another goal is to numerically verify the viscous regularization from Section 4. The nonlinear system is solved with the relative tolerance of  $10^{-14}$ . Our code is implemented in FEniCS [2], an open-source finite element library. We perform experiments using high-order Lagrange elements in space. More specifically, the SI-MEDMAC uses  $(\rho, \mathbf{u}, P) \in \mathbb{P}_2\mathbb{P}_3\mathbb{P}_2$  and the other formulations uses  $(\rho, \mathbf{u}, P) \in \mathbb{P}_3\mathbb{P}_3\mathbb{P}_2$ .

### 6.1. Accuracy test.

In this section, we verify the accuracy of the proposed formulations using a manufactured solution on a unit disk. The time step is computed using  $\text{CFL} = 0.025$  and the initial time step is used throughout the whole simulation. A small time step is chosen so that the error in time is negligible. Since the error will be dominated by spatial errors, the expected convergence rate is then 4 for velocity and 3 for pressure. The expected rate for density is 4 for all formulations except SI-MEDMAC where we expect a rate of 3. We follow the setup from [14] where the forcing function  $\mathbf{f}$  is chosen to obtain the following exact solution

$$\begin{aligned} \rho(\mathbf{x}, t) &= 2 + x \cos(\sin(t)) + y \sin(\sin(t)), \\ \mathbf{u}(\mathbf{x}, t) &= \begin{bmatrix} -y \cos(t) \\ x \cos(t) \end{bmatrix}, \\ p(\mathbf{x}, t) &= \sin(x) \sin(y) \sin(t), \\ P(\mathbf{x}, t) &= p - \alpha_\rho \rho \mathbf{u} \cdot \mathbf{u} - \frac{1}{2} \alpha_\rho \bar{\rho} \mathbf{u} \cdot \mathbf{u} - \frac{1}{|\Omega|} \int_{\Omega} \left( p - \alpha_\rho \rho \mathbf{u} \cdot \mathbf{u} - \frac{1}{2} \alpha_\rho \bar{\rho} \mathbf{u} \cdot \mathbf{u} \right) d\mathbf{x}. \end{aligned}$$



Note that we have included the modified pressure  $P$  above which is the one that is solved for in (5.1). We perform a convergence study using a series of unstructured meshes. The dynamic viscosity is set to  $\mu = 0.01$  and we set  $\kappa = 0$ . The termination time is set to  $T = 1$ .

The convergence results are presented in Figure 1 where the  $L^2$  error is plotted against the number of degrees of freedom (DOF). All the errors are computed using a high-order quadrature and are relative, i.e., they are normalized with their corresponding norm. Overall, the velocity errors converge with the expected convergence rate 4 and all formulations have similar errors. Similarly, the pressure errors converge with the expected rate of 3 with similar errors for all formulations. However, for density, the convergence rate drops to around 3.5 for all formulations except the LSI-EMAC formulation. The reason for this is that the added term in the density update  $\alpha_\rho(\nabla \cdot \mathbf{u})(\rho - \bar{\rho})$  pollutes the accuracy of  $\rho$ . If  $\mathbf{u}$  has an error  $\mathcal{O}(h^4)$ , then  $\nabla \cdot \mathbf{u} = \mathcal{O}(h^3)$ . This means that a  $\mathcal{O}(h^3)$  perturbation has been added to the density update and this explains why density converges with a suboptimal rate of  $\approx 3.5$  instead of 4. Even though the SI-MEDMAC uses  $\rho \in \mathbb{P}_2$ , we observe that it converges with the superoptimal rate  $\approx 3.5$ . SI-MEDMAC is the most accurate formulation for density even though it uses a lower polynomial degree.

Another important observation is that the shift-invariant formulations are more accurate than their counterpart, i.e., SI-EDMAC is more accurate than EDMAC, and SI-MEMAC is more accurate than MEMAC. More specifically, the error for density is roughly 1 order of magnitude lower for SI compared to the non-SI formulations.

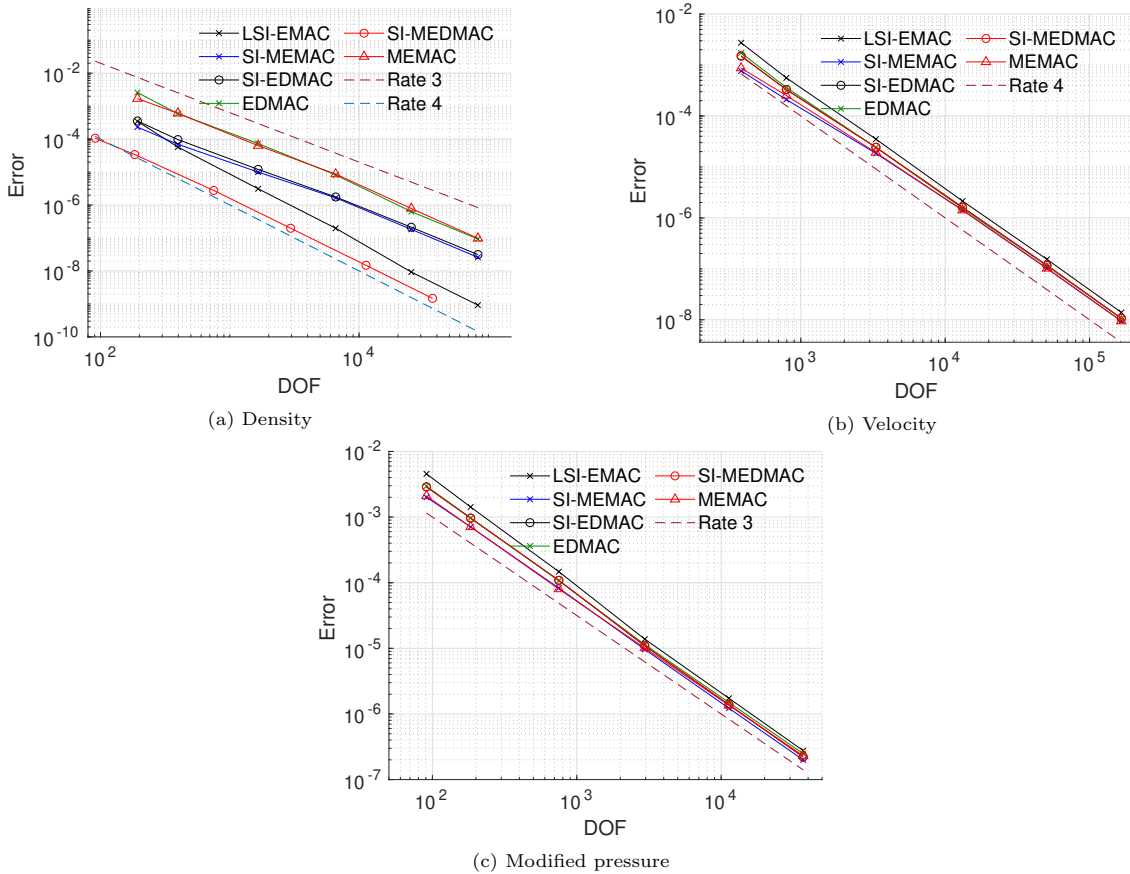


Figure 1: Manufactured solution. Relative  $L^2$ -error versus degrees of freedom. Convergence study for  $T = 1$ ,  $\mu = 0.01$ ,  $\text{CFL} = 0.025$ . All formulations used  $(\rho, \mathbf{u}, P) \in \mathbb{P}_3\mathbb{P}_3\mathbb{P}_2$ , except SI-MEDMAC which used  $(\rho, \mathbf{u}, P) \in \mathbb{P}_2\mathbb{P}_3\mathbb{P}_2$ .

### 6.2. Gresho problem with variable density.

In this section, we numerically verify the conserved properties of the formulations under investigation (see Table 2) for the inviscid case. To this end, we consider the so-called Gresho problem which was originally conceived for constant density incompressible flow [10]. We modify the problem so that density is variable and obtain the following exact solution

$$\begin{aligned} \rho &= 5 + 0.1 \left( 1 - \tanh \left( \frac{x^2 + y^2}{r_0^2} - 1 \right) \right), \\ r \leq 0.2 : & \begin{cases} \mathbf{u} = \begin{pmatrix} -5y \\ 5x \end{pmatrix}, \\ p = 12.5r^2 + C_1 \end{cases}, \\ r > 0.4 : & \begin{cases} \mathbf{u} = \begin{pmatrix} 0 \\ 0 \end{pmatrix}, \\ p = 0 \end{cases}, \\ 0.2 \leq r \leq 0.4 : & \begin{cases} \mathbf{u} = \begin{pmatrix} \frac{-2y}{r} + 5y \\ \frac{2x}{r} - 5x \end{pmatrix}, \\ p = 12.5r^2 - 20r + 4 \log(r) + C_2 \end{cases}, \end{aligned}$$

where  $r = \sqrt{x^2 + y^2}$  and we set  $r_0 = 1/8$  and

$$C_2 = (-12.5)(0.4)^2 + 20(0.4)^2 - 4 \log(0.4), C_1 = C_2 - 20(0.2) + 4 \log(0.2).$$

The main difficulty with this benchmark is that velocity is non-smooth at  $r = 0.2$  and  $r = 0.4$ , which will make  $\nabla \cdot \mathbf{u} \neq 0$  even when  $h \rightarrow 0$ . This means that the problem will test if the numerical scheme can conserve the properties considered in this work even when the divergence-free condition is severely violated. To be able to run the simulations longer without code crashes due to positivity issues, the density profile was chosen to be smooth. It is important to emphasize that a stabilized scheme for the incompressible variable density Euler equations would be able to solve this problem without numerical instabilities. Since the purpose of this test is to verify Table 1 numerically, no stabilization is used. We use a coarse mesh (4705  $\mathbb{P}_3$  and 2113  $\mathbb{P}_2$  nodes). The time step is computed using CFL = 0.5 and the initial time step is used throughout the whole simulation. The slip boundary condition is used on all boundaries.

The results are presented in Figure 2 and show that the proved properties agree with the numerical results. The minimum of  $\rho$  is computed node-wise and the  $L^2$  errors are not normalized. More specifically, we observe that kinetic energy, momentum and angular momentum are conserved for all EMAC formulations. There are some small violations of this because numerical errors spread to the boundary (where slip is imposed strongly) and when density is close to the vacuum stage. In Figure 2, by ‘*Squared density\**’ we refer to the modified energy of the advection equation given by  $\int_{\Omega} \rho^2 d\mathbf{x} - \frac{1}{|\Omega|} \left( \int_{\Omega} \rho d\mathbf{x} \right)^2$ .

One important observation is that the shift-invariant property plays a big role, where the shift-invariant formulations are the most robust. For instance, compare SI-MEMAC and SI-EDMAC to MEMAC and EDMAC. The SI-EDMAC and SI-MEDMAC formulations are the most robust and the only formulations that avoided code crash. The SI-MEDMAC formulation is the most accurate for density even though it used fewer degrees of freedom, i.e., 2113  $\mathbb{P}_2$  nodes compared to 4705  $\mathbb{P}_3$  nodes.

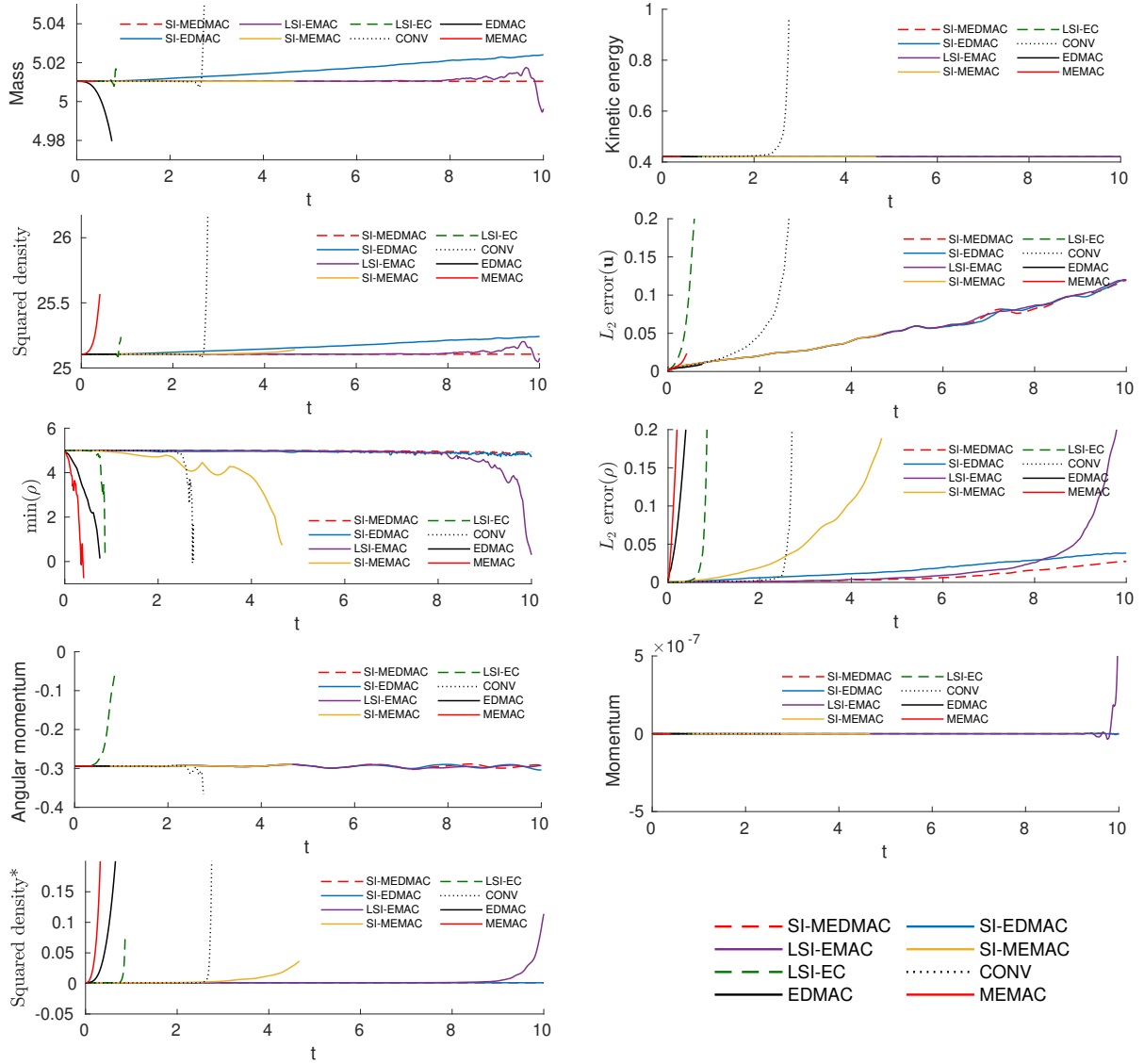


Figure 2: Gresho problem with variable density using CFL = 0.5 and 4705  $\mathbb{P}_3$  nodes.  $\kappa = \nu = \mu = 0$ . No stabilization is used. All formulations used  $(\rho, \mathbf{u}, P) \in \mathbb{P}_3\mathbb{P}_3\mathbb{P}_2$ , except SI-MEDMAC which used  $(\rho, \mathbf{u}, P) \in \mathbb{P}_2\mathbb{P}_3\mathbb{P}_2$ .

### 6.3. Viscous test.

In this test, we numerically verify the properties of the viscous regularization. Since we are only interested in the properties of the model and not the discretization, we modify the Gresho problem from Section 6.2 so that  $\mathbf{u}$  is smooth, meaning that  $\nabla \cdot \mathbf{u} \rightarrow 0$  as  $h \rightarrow 0$ . This means that for a fine mesh, the divergence-free condition will not affect the conserved properties much. The only factor that will meaningfully affect the computed properties is viscous regularization. We consider the following initial condition

$$\begin{aligned}
 \rho &= 1 + 0.5 \left( 1 - \tanh \left( \frac{x^2 + y^2}{r_0^2} - 1 \right) \right), \\
 \mathbf{u} &= 0.1 \left( 1 - \tanh \left( \frac{x^2 + y^2}{r_0^2} - 1 \right) \right) \begin{pmatrix} -5y \\ 5x \end{pmatrix},
 \end{aligned} \tag{6.1}$$

on the domain  $\Omega = \{(x, y) \in (-1.25, -1.25) \times (1.25, 1.25)\}$  using periodic boundary conditions. The initial condition (6.1) is an exact solution iff  $\kappa = \mu = 0$ . For  $\mu \neq 0$  or  $\kappa \neq 0$ , the analytic solution is not known. We are interested in the behavior of the solution when  $\kappa > 0$  and  $\mu = 0$  since we want to verify Theorem 4.1. If  $\mu = 0$ , the first condition of Theorem 4.1 is equivalent to kinetic energy conservation.

We set  $r_0 = 0.125$ ,  $\kappa = 0.01$ ,  $\mu = 0$ . The time step is computed using  $\text{CFL} = 0.2$  and the initial time step is used throughout the whole simulation. We use a fine mesh (73728  $\mathbb{P}_3$  nodes) so that the discretization error is small since we are only interested in the viscous contribution. Since the discretization error is small, the formulations in Table 2 will produce very similar results. We use the SI-MEDMAC formulation.

The results are presented in Figure 3 using three different viscous regularizations (4.7)-(4.8). The results agree with the theory, i.e.,

- $\mathbf{f}_{GP}$  conserves kinetic energy and momentum but not angular momentum.
- $\mathbf{f}_{KS}$  and  $\mathbf{f}_0$  conserve momentum and angular momentum but not kinetic energy.

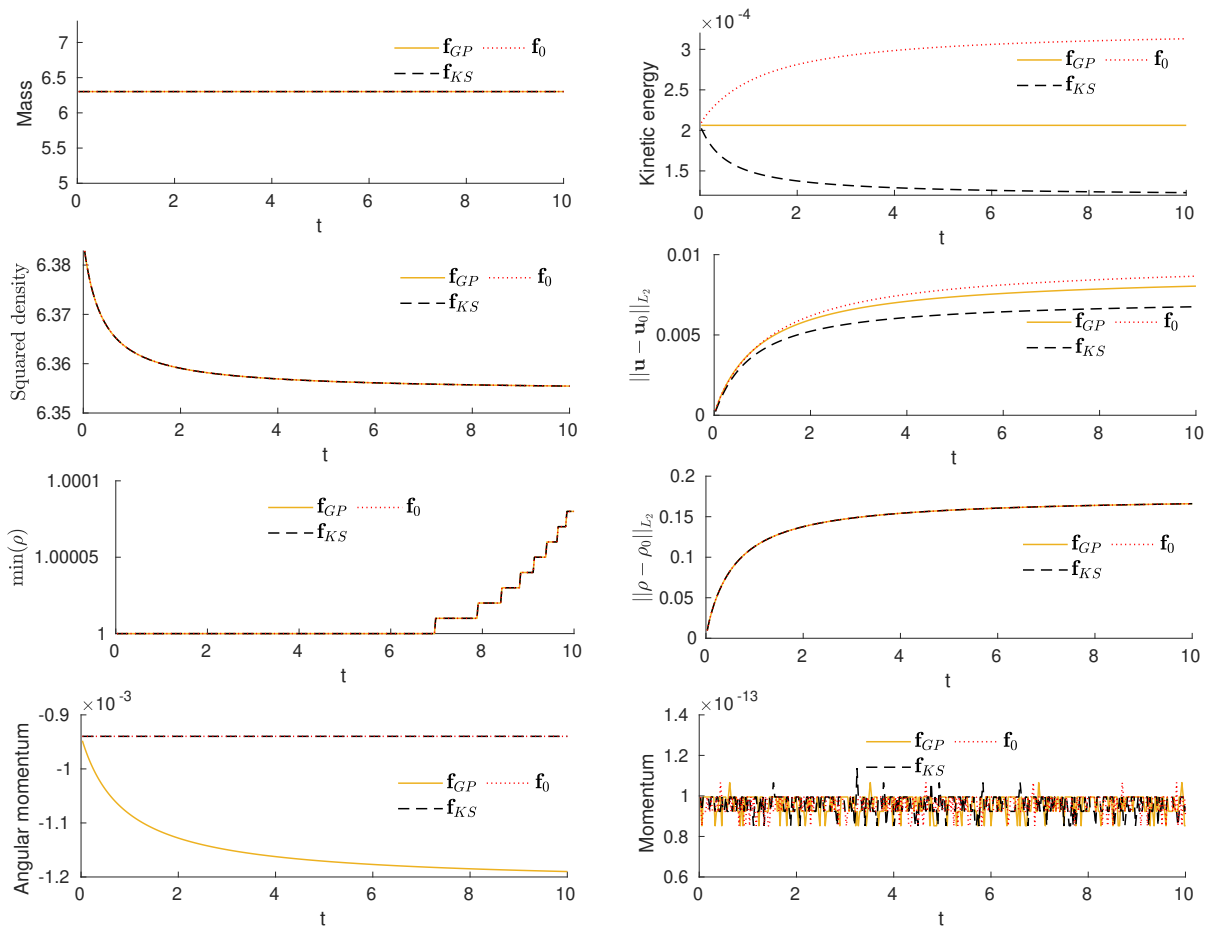


Figure 3: Comparison of viscous regularizations (4.7)-(4.8) using  $\mu = \nu = 0$ ,  $\kappa = 0.01$  for a smooth variant of the Gresho problem with variable density and periodic boundary conditions. The solution was obtained using  $\text{CFL} = 0.2$ , 73728  $\mathbb{P}_3$  nodes and no stabilization was used.

#### 6.4. Lock-exchange 2D.

In this section, we compare some different viscous regularizations for a more realistic problem. The problem we consider is the so-called lock-exchange problem which was studied extensively by Bartholomew

and Laizet [3] and Birman et al. [4]. The reason why this problem is of interest to us is that it is one of the few case studies in the variable density flow literature which includes mass diffusivity in the model, i.e.,  $\kappa > 0$ . The classical setup is a heavy fluid with density  $\rho_1$  and a lighter fluid with density  $\rho_2$  separated by a vertical barrier. The heavy fluid is located to the left of the barrier and the lighter fluid is to the right. The barrier is removed at  $t = 0$  and then the heavy gas moves to the right and the lighter fluid moves to the left. Following the setup from [3, 4], the computational domain is set to  $\Omega = \{(x, y) \in (-L/2, L/2) \times (0, 32L)\}$  with a characteristic velocity scale set to  $u = \sqrt{g(\rho_1 - \rho_2)/\rho_1 L}$  and the Reynolds number is defined as  $Re = \rho_1 L^{3/2} \sqrt{g(\rho_1 - \rho_2)/\rho_1}/\mu$ . Following the reference we set  $L = 1$ ,  $\rho_2 = 0.7$  and  $\rho_1 = 1.0$ . The Reynolds number is set to 4000 yielding a constant kinematic viscosity coefficient  $\nu$ . In summary, we set  $\mu = \rho\nu$ . The forcing function is set to  $\mathbf{f} = (0, -\rho g)$  with  $g = 1$  to yield a downward gravitational force. The initial condition is initially regularized using the error function and is given by

$$\rho^0(\mathbf{x}) = \frac{1}{2} \left( \frac{\rho_2}{\rho_1} + 1 \right) - \frac{1}{2} \left( 1 - \frac{\rho_2}{\rho_1} \right) \operatorname{erf} \left( x_0 \sqrt{Re} \right),$$

where  $x_0 = 14$  is the location of the barrier at  $t = 0$ . Following the reference, the mass diffusivity coefficient is set to  $\kappa = \nu$  which means that the so-called Schmidt number which governs the relation of molecular diffusivity and kinematic viscosity is set to 1.

The computed densities are presented in Figures 4 - 6 at times  $T = 1, 3, 5, 7, 10$  (at time-scale  $L^{1/2} (g(\rho_1 - \rho_2)/\rho_1)^{-1/2}$ ). The contour lines at the final time step are plotted in Figure 7. The results were computed using the SI-MEDMAC formulation using 1851121  $\mathbb{P}_3$  nodes on a uniform mesh. The parameters for the time-stepping are set to  $CFL = 0.1$ ,  $s_{max} = 1.02$ ,  $s_{min} = 0.98$ . The results using the momentum and angular momentum conserving viscous flux  $\mathbf{f}_0$  match with the reference [3, Fig 4] since we use the same viscous flux on a fine mesh. In Appendix B we extend the benchmark to 3D.

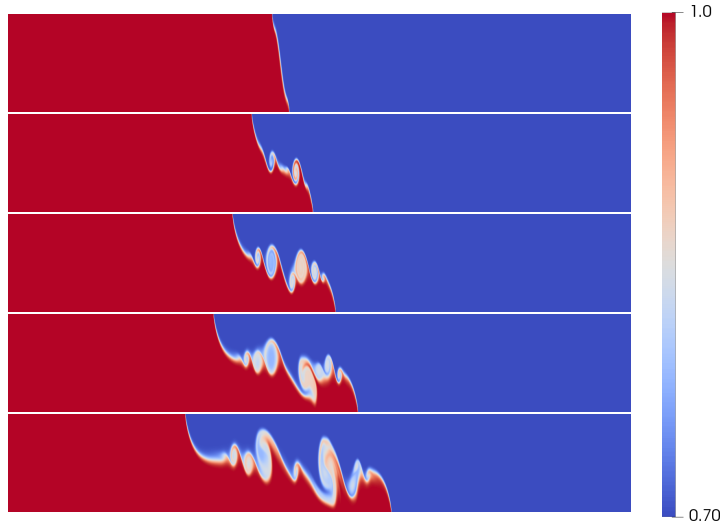


Figure 4: Momentum and angular momentum conserving viscous flux:  $\mathbf{f}_0$ . Lock-exchange problem at  $Re = 4000$ , Schmidt number 1 and density ratio 1/0.7. Density  $\rho$  at times  $t = 1, 3, 5, 7, 10$ .

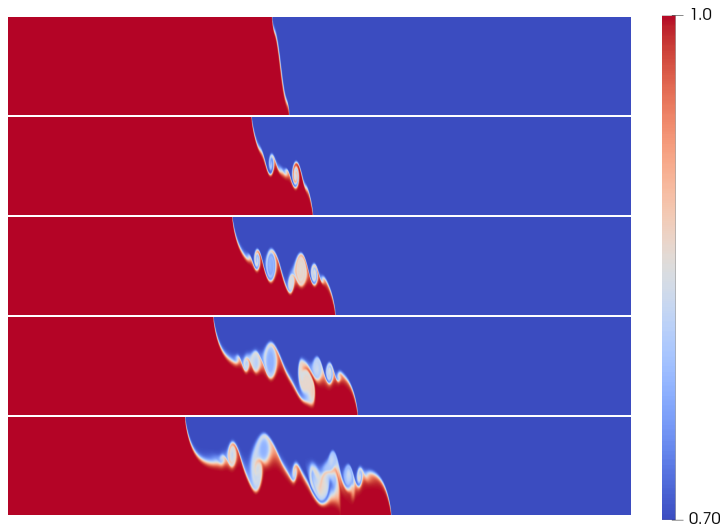


Figure 5: Momentum and angular momentum conserving viscous flux:  $\mathbf{f}_{KS}$ . Lock-exchange problem at  $Re = 4000$ , Schmidt number 1 and density ratio  $1/0.7$ . Density  $\rho$  at times  $t = 1, 3, 5, 7, 10$ .

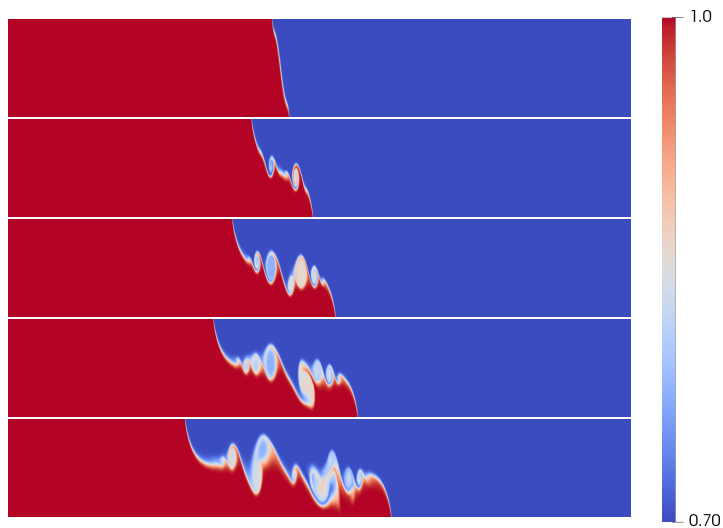


Figure 6: Guermond-Popov viscous flux:  $\mathbf{f}_{GP}$ . Lock-exchange problem at  $Re = 4000$ , Schmidt number 1 and density ratio  $1/0.7$ . Density  $\rho$  at times  $t = 1, 3, 5, 7, 10$ .

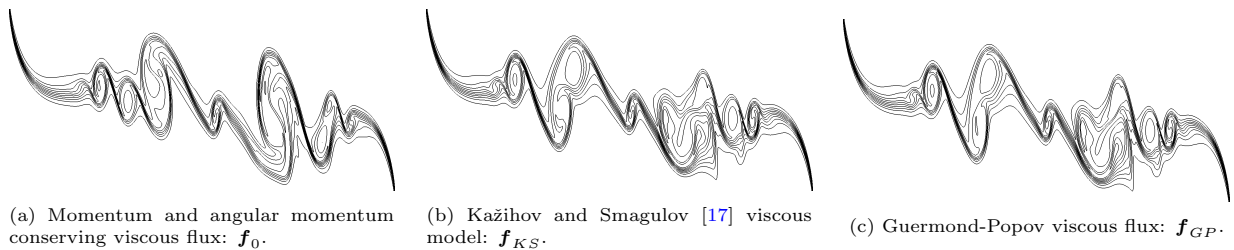


Figure 7: Lock-exchange problem at  $Re = 4000$ , Schmidt number 1 and density ratio  $1/0.7$ . Contour lines of density at  $T = 10$  for three different viscous regularizations.

## 7. Conclusion.

By modifying the governing equations in a consistent way, we introduce a new formulation for the incompressible variable density Navier-Stokes equations that, when discretized by a Galerkin method, is shift-invariant and mass, squared density, kinetic energy, momentum and angular momentum conserving (SI-MEDMAC). The formulation we propose for the inviscid case (2.1) is

$$\begin{aligned} \partial_t \rho + \mathbf{u} \cdot \nabla \rho + \frac{1}{2} (\nabla \cdot \mathbf{u}) (\rho - \bar{\rho}) &= 0, \\ \partial_t \mathbf{m} + \mathbf{u} \cdot \nabla \mathbf{m} + (\nabla \cdot \mathbf{u}) \mathbf{m} + \nabla P + (\nabla \mathbf{u}) \mathbf{m} \\ (\nabla \mathbf{m}) \mathbf{u} + \frac{1}{2} \left( \nabla \rho (\mathbf{u} \cdot \mathbf{u}) - \frac{1}{2} \nabla ((\rho - \bar{\rho}) \mathbf{u} \cdot \mathbf{u}) \right) &= \mathbf{f}, \end{aligned}$$

where  $P = p - \frac{1}{4} \rho \mathbf{u} \cdot \mathbf{u} - \frac{1}{4} \bar{\rho} \mathbf{u} \cdot \mathbf{u}$  is a modified pressure and  $\bar{\rho} = \frac{1}{|\Omega|} \int_{\Omega} \rho \, d\mathbf{x}$ . If  $\rho = 1$ , the formulation simplifies to the EMAC formulation by Charnyi et al. [5]. One important finding is that by ensuring that the polynomial degree of the mixed FEM formulation satisfies  $k_{\rho} \leq k_P$ , mass conservation is automatically achieved. Similarly, by setting  $2k_{\rho} \leq k_P$ , squared density conservation can be automatically achieved. We numerically compare the new formulation to some previously considered in the literature (see Table 2). The new formulation performs the best on the benchmarks considered in this manuscript, both in terms of accuracy for smooth problems and in terms of robustness.

Lastly, we consider the effect of viscous regularizations and our theoretical findings are summarized in Theorem 4.1. One implication of Theorem 4.1 is that, if mass diffusion is included in the model, there is no viscous regularization that simultaneously dissipates kinetic energy and conserves angular momentum. Another implication is that a unique viscous regularization dissipates kinetic energy and conserves momentum.

As additional work, one could extend the formulation to more realistic multiphase flow models where surface tension is included such as Cahn-Hilliard or similar. One interesting research direction would be to consider positivity-preserving discretizations that are also shift-invariant. It would also be interesting to investigate which viscous regularization in Section 4 gives the best match with experimental data from real-world experiments. For underresolved flows, i.e.,  $\kappa \ll h$  or  $\mu \ll h$ , we recommend that a stabilization technique [28, 20, 22, 23] is used.

## Acknowledgments.

The computations were enabled by resources in project SNIC 2022/22-428 provided by the Swedish National Infrastructure for Computing (SNIC) at UPPMAX, partially funded by the Swedish Research Council through grant agreement no. 2018-05973. The first author was partly supported by the Center for Interdisciplinary Mathematics, Uppsala University.

## Appendix A. Different formulations of the model problem

Since it is common to write the governing equations in primitive form, we reiterate the results of this manuscript for the governing equations below

$$\begin{aligned} \partial_t \rho + \mathbf{u} \cdot \nabla \rho &= \nabla \cdot \mathbf{f}_{\rho}, \\ \rho \partial_t \mathbf{u} + \mathbf{m} \cdot \nabla \mathbf{u} + \nabla p &= \mathbf{f} + \nabla \cdot (\mu (\nabla \mathbf{u} + (\nabla \mathbf{u})^{\top})) + \mathbf{f}_{\mathbf{m}} - (\nabla \cdot \mathbf{f}_{\rho}) \mathbf{u}, & (\mathbf{x}, t) \in \Omega \times (0, T], \\ \nabla \cdot \mathbf{u} &= 0, & \\ \mathbf{u}(\mathbf{x}, 0) &= \mathbf{u}_0(\mathbf{x}), \\ \rho(\mathbf{x}, 0) &= \rho_0(\mathbf{x}), & \mathbf{x} \in \Omega. \end{aligned} \tag{A.1}$$

Similarly, it is also common to write the time-derivative as  $\sqrt{\rho}\partial_t(\sqrt{\rho}\mathbf{u})$  [13] instead of  $\partial_t\mathbf{m}$  which leads to

$$\begin{aligned}
& \partial_t\rho + \mathbf{u}\cdot\nabla\rho = \nabla\cdot\mathbf{f}_\rho, \\
& \sqrt{\rho}\partial_t(\sqrt{\rho}\mathbf{u}) + \frac{1}{2}\mathbf{u}\cdot\nabla\mathbf{m} + \frac{1}{2}\mathbf{m}\cdot\nabla\mathbf{u} + \nabla p = \mathbf{f} + \nabla\cdot(\mu(\nabla\mathbf{u} + (\nabla\mathbf{u})^\top)) \\
& \quad + \mathbf{f}_m - \frac{1}{2}(\nabla\cdot\mathbf{f}_\rho)\mathbf{u}, \quad (\mathbf{x}, t) \in \Omega \times (0, T], \quad (\text{A.2}) \\
& \nabla\cdot\mathbf{u} = 0, \\
& \mathbf{u}(\mathbf{x}, 0) = \mathbf{u}_0(\mathbf{x}), \\
& \rho(\mathbf{x}, 0) = \rho_0(\mathbf{x}), \quad \mathbf{x} \in \Omega.
\end{aligned}$$

Many Navier-Stokes solvers use these formulations as their starting point and all the theoretical results of this manuscript directly translate to these forms provided that the formulations are modified accordingly. For instance, Theorem 4.1 holds for the above formulations since the term  $(\nabla\cdot\mathbf{f}_\rho)\mathbf{u}$  is included. Additionally, all the conservativeness given when  $\nabla\cdot\mathbf{u} \neq 0$  holds provided the formulations are slightly modified, see the forthcoming sections.

#### Appendix A.1. Velocity formulation.

If solving the problem in primitive form (A.1) is preferred we propose the following formulation: Find  $(\rho, \mathbf{m}, P) \in (\mathcal{M}, \mathcal{V}, \mathcal{Q})$  such that

$$\begin{aligned}
& (\rho_t, w) + (\mathbf{u}\cdot\nabla\rho, w) + \alpha_\rho((\nabla\cdot\mathbf{u})(\rho - \bar{\rho}), w) + (\kappa\nabla\rho, \nabla w) = 0, \quad \forall w \in \mathcal{M}, \\
& (\rho\mathbf{u}_t, \mathbf{v}) + b(\mathbf{m}, \mathbf{u}, \mathbf{v}) + \alpha_m((\nabla\cdot\mathbf{u})\mathbf{m}, \mathbf{u}) + (\nabla P, \mathbf{v}) \\
& + \left(\alpha_P + \frac{1}{2}\right)b(\mathbf{v}, \mathbf{m}, \mathbf{u}) + \left(\alpha_P - \frac{1}{2}\right)b(\mathbf{v}, \mathbf{u}, \mathbf{m}) - \frac{1}{2}\alpha_\rho(\nabla(\mathbf{m}\cdot\mathbf{u}), \mathbf{v}) \\
& - \frac{1}{2}((\mathbf{v}\cdot\nabla\rho, \overline{\mathbf{u}\cdot\mathbf{u}}) - \alpha_\rho(\nabla((\rho - \bar{\rho})\overline{\mathbf{u}\cdot\mathbf{u}}), \mathbf{v})) + \alpha_\rho((\nabla\cdot\mathbf{u})\bar{\rho}\mathbf{u}, \mathbf{v}) + \alpha_\rho(\nabla(\bar{\rho}\mathbf{u}\cdot\mathbf{u}), \mathbf{v}) \\
& \quad + (\mu(\nabla\mathbf{u} + (\nabla\mathbf{u})^\top), \nabla\mathbf{v}) \\
& - (\mathbf{f}, \mathbf{v}) - (\mathbf{f}_m, \mathbf{v}) - b(\kappa\nabla\rho, \mathbf{u}, \mathbf{v}) - b(\kappa\nabla\rho, \mathbf{v}, \mathbf{u}) = 0, \quad \forall \mathbf{v} \text{ in } \mathcal{V}, \\
& (\nabla\cdot\mathbf{u}, q) = 0, \quad \forall q \in \mathcal{Q},
\end{aligned} \tag{A.3}$$

where  $P = p - \alpha_P\rho\mathbf{u}\cdot\mathbf{u} - \frac{1}{2}\alpha_\rho\bar{\rho}\mathbf{u}\cdot\mathbf{u}$ . Note that integration by parts was performed on  $(\nabla\cdot\mathbf{f}_\rho)\mathbf{u}$  inside (A.1). The properties of (A.3) are summarized in Table A.4 and Table 1.

#### Appendix A.2. Fully discrete approximation.

Similar to Section 5 the standard Crank-Nicolson method can be applied on (A.3).  $\rho\mathbf{u}_t$  is discretized as  $\frac{\rho^{n+1/2}(\mathbf{u}^{n+1} - \mathbf{u}^n)}{\Delta t_n}$  and  $\overline{\mathbf{u}\cdot\mathbf{u}}$  is discretized as  $\overline{\mathbf{u}^{n+1/2}\cdot\mathbf{u}^{n+1/2}}$ . This leads to all properties at the fully discrete level except kinetic energy. By instead discretizing  $\overline{\mathbf{u}\cdot\mathbf{u}}$  and  $\frac{1}{2}(|\mathbf{u}^n|^2 + |\mathbf{u}^{n+1}|^2)$  all properties except momentum and angular momentum are fulfilled.

#### Appendix A.3. Mixed formulation.

If solving the problem in the mixed form (A.2) is preferred we propose the following formulation: Find  $(\rho, \mathbf{m}, P) \in (\mathcal{M}, \mathcal{V}, \mathcal{Q})$  such that



$$\begin{aligned}
& (\rho_t, w) + (\mathbf{u} \cdot \nabla \rho, w) + \alpha_\rho ((\nabla \cdot \mathbf{u})(\rho - \bar{\rho}), w) = 0, \quad \forall w \in \mathcal{M}, \\
& (\sqrt{\bar{\rho}}(\sqrt{\bar{\rho}}\mathbf{u})_t, \mathbf{v}) + \frac{1}{2}(b(\mathbf{m}, \mathbf{u}, \mathbf{v}) + b(\mathbf{u}, \mathbf{m}, \mathbf{v})) + \alpha_m ((\nabla \cdot \mathbf{u})\mathbf{m}, \mathbf{u}) + (\nabla P, \mathbf{v}) \\
& \quad + \alpha_P b(\mathbf{v}, \mathbf{m}, \mathbf{u}) + \alpha_P b(\mathbf{v}, \mathbf{u}, \mathbf{m}) + \frac{1}{2}\alpha_\rho ((\nabla \cdot \mathbf{u})\bar{\rho}\mathbf{u}, \mathbf{v}) + \frac{1}{2}\alpha_\rho (\nabla(\bar{\rho}\mathbf{u} \cdot \mathbf{u}), \mathbf{v}) \\
& \quad \quad \quad + (\mu(\nabla \mathbf{u} + (\nabla \mathbf{u})^\top), \nabla \mathbf{v}) \\
& = (\mathbf{f}, \mathbf{v}) + (\mathbf{f}_m, \mathbf{v}) + \frac{1}{2}(b(\kappa \nabla \rho, \mathbf{u}, \mathbf{v}) + b(\kappa \nabla \rho, \mathbf{v}, \mathbf{u})) = 0, \quad \forall \mathbf{v} \text{ in } \mathcal{V}, \\
& \quad \quad \quad (\nabla \cdot \mathbf{u}, q) = 0, \quad \forall q \in \mathcal{Q},
\end{aligned} \tag{A.4}$$

where  $P = p - \alpha_P \mathbf{m} \cdot \mathbf{u} - \frac{1}{2}\alpha_\rho \bar{\rho} \mathbf{u} \cdot \mathbf{u}$ . Note that integration by parts was performed on  $(\nabla \cdot \mathbf{f}_\rho)\mathbf{u}$  inside (A.1). The properties of (A.4) are summarized in Table A.4 and Table 1.

#### Appendix A.4. Fully discrete approximation

Similar to Section 5 the standard Crank-Nicolson method can be applied on (A.4).  $\sqrt{\bar{\rho}}(\sqrt{\bar{\rho}}\mathbf{u})_t$  is discretized as  $\rho^{n+1/2} \frac{\mathbf{u}^{n+1} - \mathbf{u}^n}{\Delta t_n} + \frac{1}{2} \mathbf{u}^{n+1/2} \frac{\rho^{n+1} - \rho^n}{\Delta t_n}$  and this leads to all properties at the fully discrete level except kinetic energy.

Table A.4: Semi-discrete conservation properties for the inviscid model problem. Note that the conditions on  $\alpha_\rho, \alpha_m, \alpha_P$  are different for the different formulations.

|  | $\partial_t \int_\Omega \rho \mathbf{u} \cdot \mathbf{u} \, d\mathbf{x} = 0$ | $\partial_t \int_\Omega \mathbf{m} \, d\mathbf{x} = 0$ | $\partial_t \int_\Omega \mathbf{m} \times \mathbf{x} \, d\mathbf{x} = 0$ |
|--|--|--|--|
| $\mathbf{m}_t$ (3.3)                                     | $\alpha_m - \alpha_P - \alpha_\rho/2 = 1/2$                                  | $\alpha_m = 1$   | $\alpha_m = 1$   |
| $\sqrt{\bar{\rho}}(\sqrt{\bar{\rho}}\mathbf{u})_t$ (A.4) | $\alpha_m - \alpha_P = 1/2$  | $\alpha_\rho/2 + \alpha_m = 1$                         | $\alpha_\rho/2 + \alpha_m = 1$   |
| $\rho \mathbf{u}_t$ (A.3)                                | $\alpha_m - \alpha_P + \alpha_\rho/2 = 1/2$                                  | $\alpha_\rho + \alpha_m = 1$                           | $\alpha_\rho + \alpha_m = 1$   |

## Appendix B. Lock-exchange 3D.

In this section, we consider the lock-exchange problem in 3D. Even though the theory is developed for the Crank-Nicolson scheme, one can use the viscous regularization and formulations developed in this work with different time-integration schemes such as high-order (backward differentiation formula) BDF methods. To this end, we consider the variable time-step BDF4 method from [20] which we modify to be fully implicit.

We follow the setup of Bartholomew and Laizet [3]. The setup is similar to the 2D case with a few exceptions. No-slip boundary conditions are used on the top and bottom boundaries and slip is used on the remaining boundaries. The Reynolds number is computed in the same as in 2D, but now it is set to  $Re = 2236$  instead. The domain is set to  $\Omega = \{(x, y) \in (-1L, 17L) \times (0, 2L) \times (0, 2L)\}$ .

A random perturbation is added to the initial velocity

$$\mathbf{u}(0, \mathbf{x}) = X \cdot 0.05 \cdot \exp(-25x^2) + (0, 0, 0)^\top,$$

where  $X \sim U(-1, 1)$ , a uniform distribution of random numbers in  $(-1, 1)$ . The authors of [3] added this perturbation ‘to simulate that a physical barrier is removed’.

We compute the solution using 15,696,120  $\mathbb{P}_3$  nodes on a uniform mesh which corresponds to a similar mesh resolution as Bartholomew and Laizet [3]. We also set  $CFL = 0.1$  and use the LSI-EMAC formulation using  $\mathbb{P}_3\mathbb{P}_3\mathbb{P}_2$  elements. The nonlinear system is solved using the relative tolerance  $10^{-7}$ . The results are presented at  $T = 20$  in Figure B.8. In the figure, we compare the Guermond-Popov viscous flux ( $\mathbf{f}_{GP}$ ) and the momentum and angular momentum conserving flux that Bartholomew and Laizet [3] use ( $\mathbf{f}_0$ ). The simulations closely match Bartholomew and Laizet [3], but there is no pointwise match due to the random perturbations in the initial condition and differences in the numerical method.

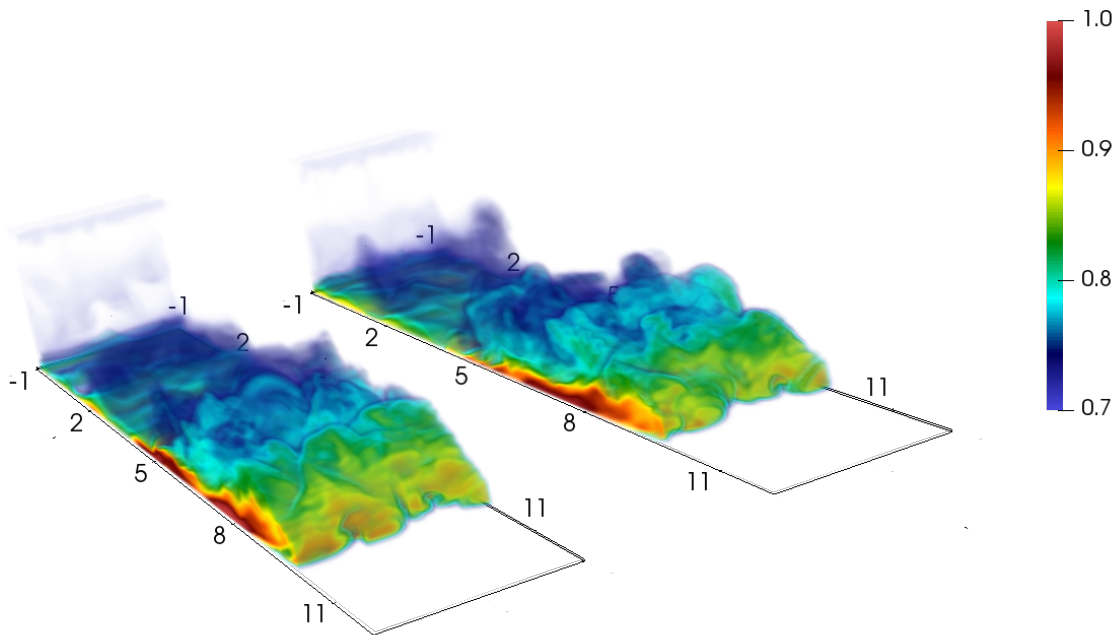


Figure B.8: Lock-exchange problem in 3D at  $Re = 2236$  and Schmidt number 1. Density  $\rho$  at  $T = 20$ . Left: Momentum and angular momentum conserving viscous flux  $\mathbf{f}_0$ . Right: Guermond-Popov viscous flux  $\mathbf{f}_{GP}$ .

## References

### References

- [1] A. S. Almgren, J. B. Bell, P. Colella, L. H. Howell, and M. L. Welcome. A conservative adaptive projection method for the variable density incompressible Navier-Stokes equations. *J. Comput. Phys.*, 142(1):1–46, 1998. ISSN 0021-9991. doi: 10.1006/jcph.1998.5890. URL <https://doi.org/10.1006/jcph.1998.5890>.
- [2] M. Alnaes, J. Blechta, J. Hake, A. Johansson, B. Kehlet, A. Logg, C. Richardson, J. Ring, M. Rognes, and G. Wells. The FEniCS project version 1.5. *Arch. Numer. Softw.*, 3:9–23, 01 2015. doi: 10.11588/ans.2015.100.20553. URL <https://doi.org/10.11588/ans.2015.100.20553>.
- [3] P. Bartholomew and S. Laizet. A new highly scalable, high-order accurate framework for variable-density flows: application to non-Boussinesq gravity currents. *Comput. Phys. Commun.*, 242:83–94, 2019. ISSN 0010-4655. doi: 10.1016/j.cpc.2019.03.019. URL <https://doi.org/10.1016/j.cpc.2019.03.019>.
- [4] V. K. Birman, J. E. Martin, and E. Meiburg. The non-Boussinesq lock-exchange problem. II. High-resolution simulations. *J. Fluid Mech.*, 537:125–144, 2005. ISSN 0022-1120. doi: 10.1017/S0022112005005033. URL <https://doi.org/10.1017/S0022112005005033>.
- [5] S. Charnyi, T. Heister, M. A. Olshanskii, and L. G. Rebholz. On conservation laws of Navier-Stokes Galerkin discretizations. *J. Comput. Phys.*, 337:289–308, 2017. ISSN 0021-9991. doi: 10.1016/j.jcp.2017.02.039. URL <https://doi.org/10.1016/j.jcp.2017.02.039>.
- [6] S. Charnyi, T. Heister, M. A. Olshanskii, and L. G. Rebholz. Efficient discretizations for the EMAC formulation of the incompressible Navier-Stokes equations. *Appl. Numer. Math.*, 141:220–233, 2019. ISSN 0168-9274. doi: 10.1016/j.apnum.2018.11.013. URL <https://doi.org/10.1016/j.apnum.2018.11.013>.
- [7] J. A. Evans and T. J. R. Hughes. Isogeometric divergence-conforming B-splines for the unsteady Navier-Stokes equations. *J. Comput. Phys.*, 241:141–167, 2013. ISSN 0021-9991. doi: 10.1016/j.jcp.2013.01.006. URL <https://doi.org/10.1016/j.jcp.2013.01.006>.
- [8] E. S. Gawlik and F. Gay-Balmaz. A conservative finite element method for the incompressible Euler equations with variable density. *J. Comput. Phys.*, 412:109439, 15, 2020. ISSN 0021-9991. doi: 10.1016/j.jcp.2020.109439. URL <https://doi.org/10.1016/j.jcp.2020.109439>.
- [9] V. Girault and P.-A. Raviart. Finite element methods for Navier-Stokes equations, volume 5 of *Springer Series in Computational Mathematics*. Springer-Verlag, Berlin, 1986. ISBN 3-540-15796-4. doi: 10.1007/978-3-642-61623-5. URL <https://doi.org/10.1007/978-3-642-61623-5>. Theory and algorithms.
- [10] P. M. Gresho and S. T. Chan. On the theory of semi-implicit projection methods for viscous incompressible flow and its implementation via a finite element method that also introduces a nearly consistent mass matrix. II. Implementation. volume 11, pages 621–659. 1990. doi: 10.1002/flid.1650110510. URL <https://doi.org/10.1002/flid.1650110510>. Computational methods in flow analysis (Okayama, 1988).

- [11] J.-L. Guermond and P. Minev. High-order adaptive time stepping for the incompressible Navier-Stokes equations. *SIAM J. Sci. Comput.*, 41(2):A770–A788, 2019. ISSN 1064-8275. doi: 10.1137/18M1209301. URL <https://doi.org/10.1137/18M1209301>.
- [12] J.-L. Guermond and B. Popov. Viscous regularization of the Euler equations and entropy principles. *SIAM J. Appl. Math.*, 74(2):284–305, 2014. ISSN 0036-1399. doi: 10.1137/120903312. URL <https://doi.org/10.1137/120903312>.
- [13] J.-L. Guermond and L. Quartapelle. A projection FEM for variable density incompressible flows. *J. Comput. Phys.*, 165(1):167–188, 2000. ISSN 0021-9991. doi: 10.1006/jcph.2000.6609. URL <https://doi.org/10.1006/jcph.2000.6609>.
- [14] J.-L. Guermond and A. Salgado. A splitting method for incompressible flows with variable density based on a pressure Poisson equation. *J. Comput. Phys.*, 228(8):2834–2846, 2009. ISSN 0021-9991. doi: 10.1016/j.jcp.2008.12.036. URL <http://dx.doi.org/10.1016/j.jcp.2008.12.036>.
- [15] W. M. Haynes. *CRC Handbook of Chemistry and Physics 2015-2016*. CRC Handbook of Chemistry & Physics. CRC Press, 96 edition, 2015. ISBN 1482260964; 9781482260960. URL [libgen.li/file.php?md5=c7c8a202cf41d366ba493814f9966517](http://libgen.li/file.php?md5=c7c8a202cf41d366ba493814f9966517).
- [16] S. Ingimarnson, M. Neda, L. G. Rebholz, J. Reyes, and A. Vu. Improved long time accuracy for projection methods for Navier-Stokes equations using EMAC formulation. *International Journal of Numerical Analysis and Modeling*, 20(2):176–198, 2023. ISSN 2617-8710. doi: <https://doi.org/10.4208/ijnam2023-1008>. URL [http://global-sci.org/intro/article\\_detail/ijnam/21353.html](http://global-sci.org/intro/article_detail/ijnam/21353.html).
- [17] A. V. Kazhlov and v. Smagulov. The correctness of boundary value problems in a certain diffusion model of an inhomogeneous fluid. *Dokl. Akad. Nauk SSSR*, 234(2):330–332, 1977. ISSN 0002-3264.
- [18] M. G. Larson and F. Bengzon. *The finite element method: theory, implementation, and applications*, volume 10 of *Texts in Computational Science and Engineering*. Springer, Heidelberg, 2013. ISBN 978-3-642-33286-9; 978-3-642-33287-6. doi: 10.1007/978-3-642-33287-6. URL <https://doi.org/10.1007/978-3-642-33287-6>.
- [19] L. Lundgren and M. Nazarov. A high-order artificial compressibility method based on Taylor series time-stepping for variable density flow. *J. Comput. Appl. Math.*, page 114846, 2022. ISSN 0377-0427. doi: <https://doi.org/10.1016/j.cam.2022.114846>. URL <https://www.sciencedirect.com/science/article/pii/S0377042722004447>.
- [20] L. Lundgren and M. Nazarov. A high-order residual-based viscosity finite element method for incompressible variable density flow, 2022. URL <https://ssrn.com/abstract=4268034>.
- [21] J. Manzanero, G. Rubio, D. A. Kopriva, E. Ferrer, and E. Valero. An entropy-stable discontinuous Galerkin approximation for the incompressible Navier-Stokes equations with variable density and artificial compressibility. *J. Comput. Phys.*, 408:109241, 32, 2020. ISSN 0021-9991. doi: 10.1016/j.jcp.2020.109241. URL <https://doi.org/10.1016/j.jcp.2020.109241>.
- [22] M. Nazarov. Convergence of a residual based artificial viscosity finite element method. *Comput. Math. Appl.*, 65(4):616–626, 2013. ISSN 0898-1221. doi: 10.1016/j.camwa.2012.11.003. URL <http://dx.doi.org/10.1016/j.camwa.2012.11.003>.
- [23] M. Nazarov and J. Hoffman. Residual-based artificial viscosity for simulation of turbulent compressible flow using adaptive finite element methods. *Internat. J. Numer. Methods Fluids*, 71(3):339–357, 2013. ISSN 0271-2091. doi: 10.1002/flid.3663. URL <http://dx.doi.org/10.1002/flid.3663>.
- [24] M. A. Olshanskii and L. G. Rebholz. Longer time accuracy for incompressible Navier-Stokes simulations with the EMAC formulation. *Comput. Methods Appl. Mech. Engrg.*, 372:113369, 17, 2020. ISSN 0045-7825. doi: 10.1016/j.cma.2020.113369. URL <https://doi.org/10.1016/j.cma.2020.113369>.
- [25] J.-H. Pyo and J. Shen. Gauge-Uzawa methods for incompressible flows with variable density. *J. Comput. Phys.*, 221(1):181–197, 2007. ISSN 0021-9991. doi: 10.1016/j.jcp.2006.06.013. URL <https://doi.org/10.1016/j.jcp.2006.06.013>.
- [26] P.-A. Raviart and J. M. Thomas. A mixed finite element method for 2nd order elliptic problems. In *Mathematical aspects of finite element methods* (Proc. Conf., Consiglio Naz. delle Ricerche (C.N.R.), Rome, 1975), *Lecture Notes in Math.*, Vol. 606, pages 292–315. Springer, Berlin, 1977.
- [27] L. R. Scott and M. Vogelius. Conforming finite element methods for incompressible and nearly incompressible continua. In *Large-scale computations in fluid mechanics, Part 2* (La Jolla, Calif., 1983), volume 22 of *Lectures in Appl. Math.*, pages 221–244. Amer. Math. Soc., Providence, RI, 1985. doi: 10.1051/m2an/1985190101111. URL <https://doi.org/10.1051/m2an/1985190101111>.
- [28] V. Stiernström, L. Lundgren, M. Nazarov, and K. Mattsson. A residual-based artificial viscosity finite difference method for scalar conservation laws. *J. Comput. Phys.*, 430:Paper No. 110100, 29, 2021. ISSN 0021-9991. doi: 10.1016/j.jcp.2020.110100. URL <https://doi.org/10.1016/j.jcp.2020.110100>.
- [29] Y. Zhang, H. Dong, and K. Wang. Mass, momentum and energy identical-relation-preserving scheme for the Navier-Stokes equations with variable density. *Comput. Math. Appl.*, 137:73–92, 2023. ISSN 0898-1221. doi: 10.1016/j.camwa.2023.02.004. URL <https://doi.org/10.1016/j.camwa.2023.02.004>.